

Wright State University

CORE Scholar

[Browse all Theses and Dissertations](#)

[Theses and Dissertations](#)

2012

MHC Class I Expression in Murine Fibroblast and Keratinocyte Cell Lines During the First Twenty-four Hours of Infection with Herpes Simplex Virus-1 (HSV-1)

Prasanthi Kumchala
Wright State University

Follow this and additional works at: https://corescholar.libraries.wright.edu/etd_all



Part of the [Immunology and Infectious Disease Commons](#), and the [Microbiology Commons](#)

Repository Citation

Kumchala, Prasanthi, "MHC Class I Expression in Murine Fibroblast and Keratinocyte Cell Lines During the First Twenty-four Hours of Infection with Herpes Simplex Virus-1 (HSV-1)" (2012). *Browse all Theses and Dissertations*. 596.

https://corescholar.libraries.wright.edu/etd_all/596

This Thesis is brought to you for free and open access by the Theses and Dissertations at CORE Scholar. It has been accepted for inclusion in Browse all Theses and Dissertations by an authorized administrator of CORE Scholar. For more information, please contact library-corescholar@wright.edu.

MHC class I expression in murine fibroblast and keratinocyte cell lines during the first
twenty-four hours of Infection with Herpes Simplex Virus-1 (HSV-1)

A thesis submitted in partial fulfillment of the
requirements for the degree of Master of Science

By

Prasanthi Kumchala

M.Sc., Acharya Nagarjuna University, 2006

2012

Wright State University

WRIGHT STATE UNIVERSITY

SCHOOL OF GRADUATE STUDIES

June 9, 2012

I HEREBY RECOMMEND THAT THE THESIS PREPARED UNDER MY SUPERVISION BY Prasanthi Kumchala ENTITLED MHC class I expression in murine fibroblast and keratinocyte cell lines during the first twenty-four hours of infection with Herpes Simplex Virus-1 (HSV-1) BE ACCEPTED IN PARTIAL FULFILLMENT OF THE REQUIREMENTS FOR THE DEGREE OF Master of Science

Nancy J. Bigley, Ph.D.
Thesis Director

Barbara E. Hull Ph.D.
Program Director,
Microbiology & Immunology,
College of Science & Mathematics

Committee on Final Examination

Nancy J. Bigley, Ph.D.
Professor
Microbiology & Immunology

Barbara E. Hull, Ph.D.
Professor of Biological Sciences

Gerald M. Alter, Ph.D.
Professor, Department of Biochemistry
& Molecular Biology

Andrew T Hsu, Ph.D.
Dean, Graduate School

ABSTRACT

Kumchala Prasanthi. M.S., Department of Microbiology and Immunology, Wright State University, 2012. MHC class I expression in murine fibroblast and keratinocyte cell lines during the first twenty-four hours of Infection with Herpes Simplex Virus-1 (HSV-1).

The hypothesis of this study is: HSV-1 infection of murine fibroblasts and keratinocytes inhibits expression of MHC class I molecules during first 24 hours of infection. IFN- γ pretreatment of fibroblasts protected the cells from virus-induced inhibition of MHC class I expression, but did not protect keratinocytes. Herpesviruses are known for their ability to establish persistent infections. Herpesviruses exert many different ways to suppress host defense mechanisms. One such way is by down regulating expression of the major histocompatibility complex I (MHC I) molecules in infected cells. Epidermal cells such as keratinocytes are the major sites for herpes simplex virus type 1 (HSV-1) replication both in active primary and recurring herpes infection. In this study, murine keratinocyte cell lines (HEL-30 & PAM-212) were shown to be refractory to IFN- γ induction of an MHC class I expression to HSV-1 infection, while IFN- γ did induce MHC class I expression in murine fibroblast cell lines (L929 & A2R1). In the current study, using Image J analyses of immunocytochemical data, MHC class I expression decreased at 6, 12, and 24 hours after infection of L929 and A2R1 fibroblasts ($p < 0.001$) with HSV-1 infection. The effect of IFN- γ on expression of MHC I molecules was evaluated in HSV-1-infected murine keratinocytes and fibroblasts at 24 hours after infection. In other studies, IFN- γ was found to protect the murine fibroblast cell line, L929 from the cytopathic effect of HSV-1 but was unable to protect murine

keratinocyte cell lines (HEL-30 and PAM-212) from HSV-1 induced cytopathic effects (Frey et al., 2009). Immunofluorescent staining for expression of MHC class I molecules in IFN- γ treated and HSV-1 infected cells was performed using immunocytochemistry and flow cytometry. Only the fibroblast cell lines could be examined by both methods. Significant increases ($p < 0.001$) in expression of MHC class I molecules were seen in both HSV-1 infected fibroblast cell lines after treatment with IFN- γ using both immunocytochemistry and flow cytometry. Since keratinocytes grow in clusters, immunocytochemistry was not used to evaluate their expression of the MHC class I molecules in HSV-1-infected and IFN- γ treated cells. Keratinocytes could be gently removed from the culture using cell stripper solution, and were then examined by flow cytometry for expression of MHC class I molecules. In both keratinocyte cell lines, significant decreases in expression levels of MHC class I molecules over baseline levels ($p < 0.001$) were observed after HSV-1 infection and IFN- γ treatment.

In the current study, HSV-1 infection of murine fibroblasts and keratinocytes inhibited expression of MHC class I molecules during first 24 hours of infection. IFN- γ pretreatment of fibroblasts protected them from virus-induced inhibition of MHC class I expression, but did not protect keratinocytes. The refractoriness of keratinocytes to IFN- γ might be due to the expression of suppressor of cytokine synthesis-1 (SOCS-1) during HSV-1 infection as observed by the Frey et al., (2009).

TABLE OF CONTENTS

INTRODUCTION.....	1
MATERIALS AND METHODS	
Cell culture.....	14
Virus	14
IFN- γ pretreatment and virus infection of cells for immunocytochemistry.....	15
Flow cytometry.....	19
Statistical analysis.....	21
RESULTS	
Immunocytochemistry for L929 fibroblast cells.....	22
Image J quantification of MHC class I fluorescence intensity for L929 fibroblasts.....	26
Immunocytochemistry for A2R1 fibroblast cells	28
Image J quantification of MHC class I fluorescence intensity for A2R1 fibroblasts.....	32
Comparison of MHC class I fluorescence Intensity for fibroblasts at 6,12, and 24 hours post infection.....	34
MHC class I immunofluorescence intensity by Flow cytometry.....	35
MHC class I immunofluorescence intensity by Flow cytometry for L929 fibroblasts.....	36
MHC class I immunofluorescence intensity by Flow cytometry for A2R1 fibroblasts.....	38
MHC class I immunofluorescence intensity by Flow cytometry for PAM-212	

keratinocytes.....	41
MHC class I immunofluorescence intensity by Flow cytometry for HEL-30	
keratinocyte.....	43
DISCUSSION.....	48
REFERENCES.....	54

LIST OF FIGURES

Figure 1: HSV virion structure and genome organization.....	2
Figure 2: Genomic distribution of HSV glycoproteins involved in viral entry and cell-to-cell spread.....	4
Figure 3: Overview of the MHC I antigen-processing pathway	6
Figure 4: HSV1-induced fratricide of antiviral CTLs as a mechanism of viral immune evasion	7
Figure 5: Images of HEL-30 cells treated with antibodies for (a) MHC class I (green), (b) actin (red), and (c) MHC class I and actin merged	12
Figure 6: Images of trypsinized HEL-30 cells treated with antibodies for (a) MHC class I (green), (b) actin (red), and (c) MHC class I and actin merged	13
Figure 7: Immunocytochemistry for L929- 6 hours post infection MHC class I stained (Green) and actin stained (Red) images.....	23
Figure 8: Immunocytochemistry for L929- 12 hours post infection MHC class I stained (Green) and actin stained(Red) images.....	24
Figure 9: Immunocytochemistry for L929- 24 hours post infection MHC class I stained(Green) and actin stained(Red) images.	25
Figure 10: MHC class I fluorescent Intensity using image J program for L929	

fibroblasts at 6,12, and 24 hour post infection	27
Figure 11: Immunocytochemistry for A2R1- 6 hours post infection MHC class I stained(Green) and actin stained(Red) images	29
Figure 12: Immunocytochemistry for A2R1- 12 hours post infection MHC class I stained(Green) and actin stained(Red) images	30
Figure 13: Immunocytochemistry for A2R1- 24 hours post infection MHC class I stained(Green) and actin stained(Red) images	31
Figure 14: MHC class I fluorescent Intensity using image J program for A2R1 fibroblasts at 6,12, and 24 hour post infection	33
Figure 15: Comparision of MHC class I fluorescent Intensity using image J program for L929 fibroblasts at 6. 12 and 24 hour post infection time points.....	34
Figure 16: Comparision of MHC class I fluorescent Intensity using image J program for A2R1 fibroblasts at 6. 12 and 24 hour post infection time points.....	35
Figure 17: Major histocompatibility complex class I antigen expression for L929 fibroblasts through flow cytometry.....	37
Figure 18: L929 fibroblasts- Graph for flow cytometry mean fluorescent values at 24 hour post infection	38
Figure 19: Major histocompatibility complex class I antigen expression for A2R1 fibroblasts through flow cytometry	39
Figure 20: A2R1 fibroblasts- Graph for flow cytometry mean fluorescent values at 24 hour post infection	40
Figure 21: Major histocompatibility complex class I antigen expression	

for PAM-212 fibroblasts through flow cytometry	42
Figure 22: PAM-212 fibroblasts- Graph for flow cytometry mean fluorescent values at 24 hour post infection	43
Figure 23: Major histocompatibility complex class I antigen expression for HEL-30 fibroblasts through flow cytometry	45
Figure 24: HEL-30 fibroblasts- Graph for flow cytometry mean fluorescent values at 24 hour post infection	46

LIST OF TABLES

Table 1: List of treated cell groups for current study, specifying which groups are treated with IFN- γ and infected with HSV-1.....	15
Table 2: List of antibodies and isotype controls used to stain cells for immunocytochemistry and flow cytometry.....	19
Table 3: Flow cytometry results summary for Fibroblasts (L929 & A2R1) and Keratinocytes (HEL-30 & PAM-212) compared to only cells (control) at 24 hours post infection.....	47

LIST OF ABBREVIATIONS

AICD = Activation-induced cell death

BSA = Bovine serum albumen

CD95L = Cluster of differentiation 95 ligand

CTLs = Cytotoxic T cells

ER= Endoplasmic reticulum

FL cells = Human amnion cells

gB, gC, gD, gH, and gL = Glycoprotein B, C, D, H, L.

HVEM = Herpes virus entry mediator

HS = Heparin sulfate

HSV-1 = Herpes simplex virus type – 1

ICAM-1 = Intercellular Adhesion Molecule-1

ICP0 = Infected cell protein 0

ICP4 = Infected cell protein 4

IE = Immediate-early.

IFN = Interferon

IFN- α = Interferon alpha

IFN- β = Interferon beta

IFN- γ = Interferon gamma

IFNGR1 = Interferon gamma receptor 1

IFNGR2 = Interferon gamma receptor 2

IRF = Interferon regulatory factor

IL = Interleukin

ISRE = Interferon stimulated response elements

JAK = Janus-family tyrosine kinases

KIR = Kinase inhibitor region

LAT = Latency Associated Transcript

MHC class I = Major histocompatibility complex class I

MOI = Multiplicity of Infection

NGF β = Nerve growth factor

Nk = Natural killer

PFU= Plaque forming units

PKR = RNA-activated protein kinase

SOCS-1= Suppressor of cytokine signaling-1

SOCS-3 = Suppressor of cytokine signaling-3

STAT = Signal transduction and transcription

TAP = Transporter associated with antigen processing

TG = Trigeminal ganglia

TNF- α = Tumor necrosis factor- α

TS = Thymidylate synthase

ACKNOWLEDGEMENT

I would like to thank my thesis advisor Dr. Nancy Bigley for all her guidance and support that she has given me throughout my graduate study. I would also like to acknowledge and thank Dr. Barbara Hull and Dr. Gerald Alter for their timely suggestions and contributions in my work.

DEDICATION

I would like to dedicate this thesis to my husband Kiran Kumar Bandaru and my daughter Sri Amogha who have given me inspiration, encouragement and are truly a gift in my life.

Introduction

Alpha herpes viruses constitute the largest subfamily of the Herpes viridae which will cause infections to humans and animals. The human alpha herpes viruses, herpes simplex viruses type 1 (HSV-1), type 2 (HSV-2) and varicella-zoster virus (VZV) are antigenically distinct. HSV-1 can be diagnosed through oral blisters and HSV-2 through genital ulcers (Pena et al., 2010). Historically, HSV-1 was found infrequently in genital HSV infections, but recent studies show an increase in prevalence up to 60% (Marshall et al., 2001). HSV-1 also leads to infections like ocular herpes, which range from mild to severe stromal keratitis symptoms. HSV-1 may also result in blindness, encephalitis, aseptic meningitis and atypical pneumonia (Whitley, 2001).

HSV-1 is a double stranded DNA virus that causes both productive and latent infections. Latent infection can persist in the body throughout the life of the host. HSV-1 hides from the immune system by residing latently in the cell bodies of nerves. When activated, the virus will be transported to the skin from the nerves where they replicate and cause sores (Norkin, 2010). The HSV virion (Figure 1A) is comprised of the viral double-stranded DNA, an icosahedral capsid shell, a tegument layer containing numerous viral proteins and a lipid membrane envelope studded with viral glycoproteins. The HSV

genome (Figure 1B) is composed of long (L) and short (S) components with a unique region (U) flanked by inverted repeat regions (Taylor et al., 2002).

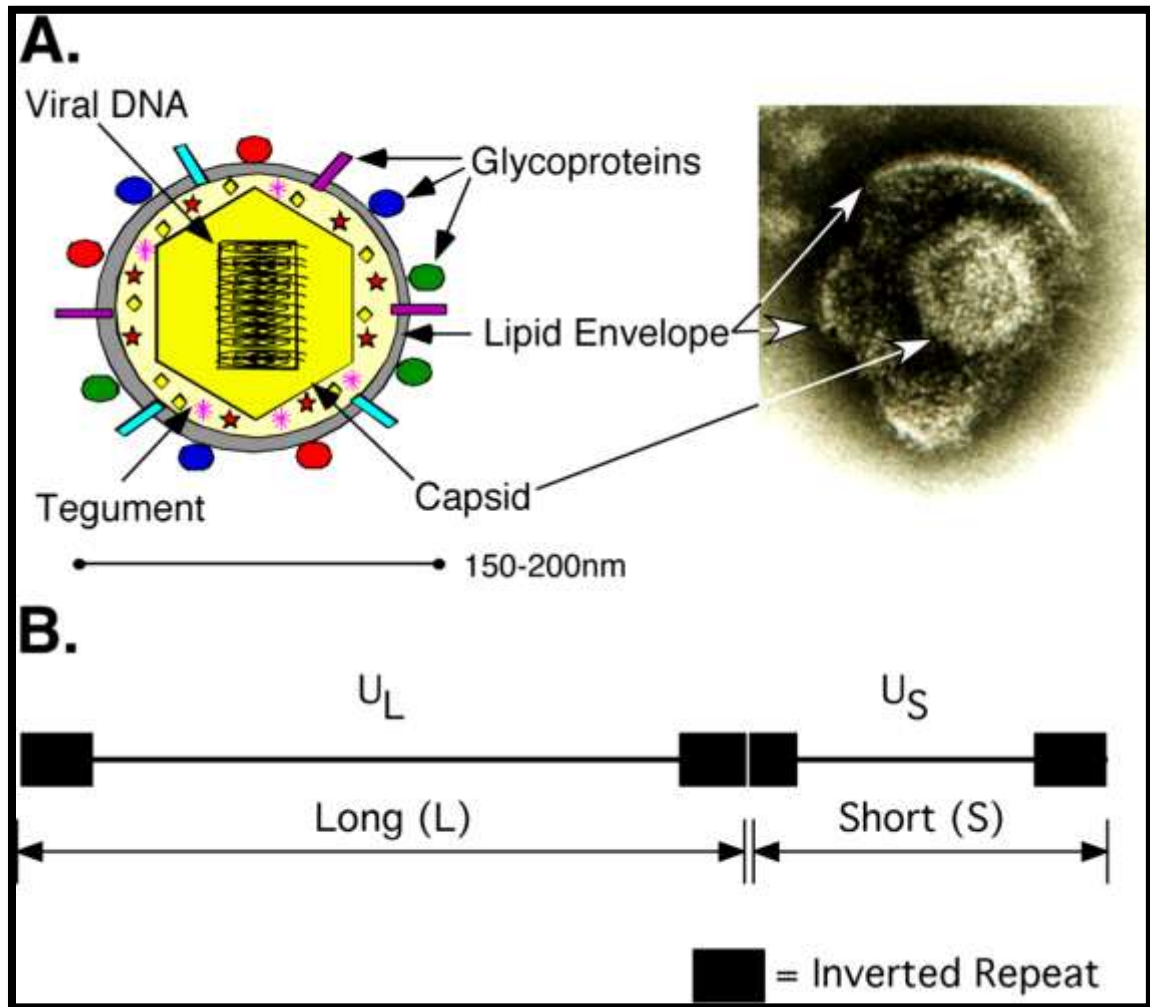


Figure 1: HSV virion structure and genome organization. The HSV virion (A), the major structural components of the virion can be seen in an EM photograph (right) where the viral envelope is ruptured and folded back. The HSV genome (B) is organized into two components, long (L) and short (S). Each component contains a unique region (U) flanked by inverted repeat regions and are linked to generate a total genome size of approximately 150,000 base pairs. (Adapted from Taylor et al., 2002).

HSV-1 utilizes glycoprotein-receptor complexes gB, gC, gD, gH, and gL during host entry and these are essential for host cell entry (Figure 2A) (Shukla et al., 2001). Initial contact and binding is made by the gC with the heparan sulfate (HS) proteoglycans on host cell surface in case of fibroblasts (Lilly et al., 1998). HSV-1 attaches using extracellular receptors in non-neuronal cells through filopodia-like membrane protrusions and reaches the cell for internalization (Figure 2B) (Oh et al., 2010). Keratinocytes are the major sites of HSV-1 replication in primary or recurring herpes infection (Cunningham et al., 2006). In particular, infection of keratinocytes occurs through endocytic processes (Figure 2B) (Nicola et al., 2005). Once fusion of the virus is completed, the viral genome enters the nucleus through the nuclear pore complex (Shahin et al., 2006). During subsequent lytic infection, the virus is able to move from the initial site of infection through the underlying strata to reach the innervating neurons (Wharton et al., 1995). Once virus traverses through neuron it establishes a latent state which is maintained by CD8⁺ T cells and IFN- γ (Hendricks et al., 1992).

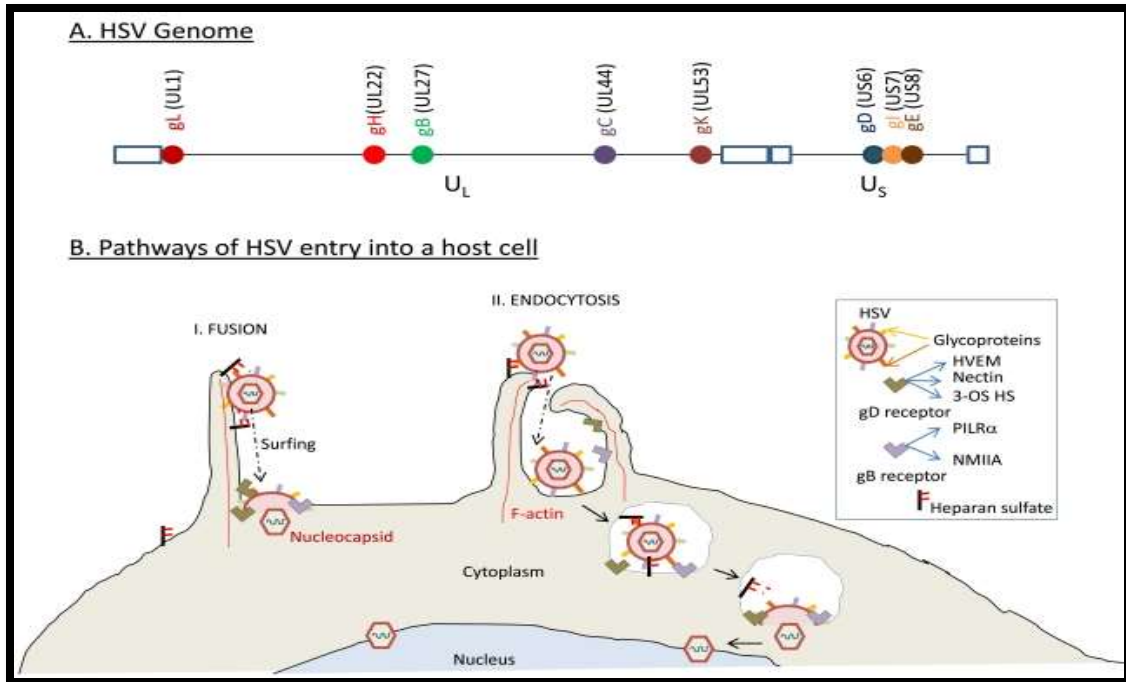


Figure 2: Genomic distribution of HSV glycoproteins involved in viral entry and cell-to-cell spread. A. Glycoprotein genes required for HSV-1 entry and spread. HSV contains a 152-kb double-stranded linear DNA genome encoding over 80 viral genes that are arranged as unique long (UL) and unique short (US) segments flanked by inverted repeat sequences (boxes). The inverted repeats contain sequences required for cleavage/packaging of the viral genome. B. Pathways of HSV entry into cells. (I) penetration by viral envelope fusion at the plasma membrane and (II) endocytosis (Adapted from Sarah et al., 2012).

The immune system plays a major role in protecting the body from infection. The system is divided into two major branches: the innate immune system and the adaptive immune system. Innate immune system is the first line of defense when the body is exposed to invading microbes. Adaptive immune system is only found in vertebrates. Assembly of antigen-binding molecules specific for structures of intracellular or extracellular pathogens takes place in adaptive immune system (Rupert and Robert, 2004).

Two types of cells present in the adaptive immune system are B cells and T cells. B cells are involved in humoral immune response and carry antigen-specific B cell receptors on their cell surface. In the presence of infection, B cells will be activated and release antibodies that bind to the antigen. T cells recognize antigenic peptides presented on the surface of host cells through major histocompatibility complex (MHC) molecules (Rupert and Robert, 2004). There are two types of MHC molecules. MHC class I molecules are found on all nucleated cell bodies and present peptides to the CD8⁺ cytotoxic T cells that kill the non-self-peptides from the pathogens. MHC class II molecules present peptides to the CD4⁺ T helper cells; these stimulate the B cells resulting in production of antibodies (Mellman and Steinman, 2001).

Major histocompatibility complex (MHC) class I molecules are becoming important targets for the virus during immune evasion. Down regulation of MHC class I expression can attenuate the CD8 T-cell-mediated recognition of infected cells. Herpes virus family members down regulate the MHC class I presentation by different mechanisms (Mark et al., 2004). Precisely, HSV-1 produces two proteins that help in inhibiting antigen attack. The first protein is a viral host shutoff protein that helps in preventing antigen production by targeting mRNA. The second protein ICP47 acts directly on the complex called TAP1/2. This complex helps in transport of antigens from cytosol to the endoplasmic reticulum (ER). Thus, when ICP47 attacks the TAP1/2 complex, then the transportation of antigens to ER will be stopped thereby affecting further functions (Mark et al., 2004). The transporter associated with antigen processing (TAP) is essential for peptide delivery from the cytosol into the lumen of the ER. These peptides are loaded to MHC class I molecules. The loaded MHC class I vacate the ER

and present the antigen on the cell surface of cytotoxic T cells (CTLs). Interaction of cytotoxic T cells leads to the elimination of virus infected cells (Figure 3) (Rupert and Robert, 2004).

Raftery et al., proposed a mechanism underlying fratricide in active HSV-1 infections. During HSV-1 infection on epithelial cells, free virions can bind to herpes virus entry mediator (HVEM) molecule and infect the CTLs. These CTLs, when they recognize the viral antigen will up regulate the CD95L. During this time, HSV-1 blocks AICD and down regulates MHC class I molecules. This overall mechanism makes CTLs more susceptible to infection than epithelial cells (Figure 4) (Raftery et al., 1999).

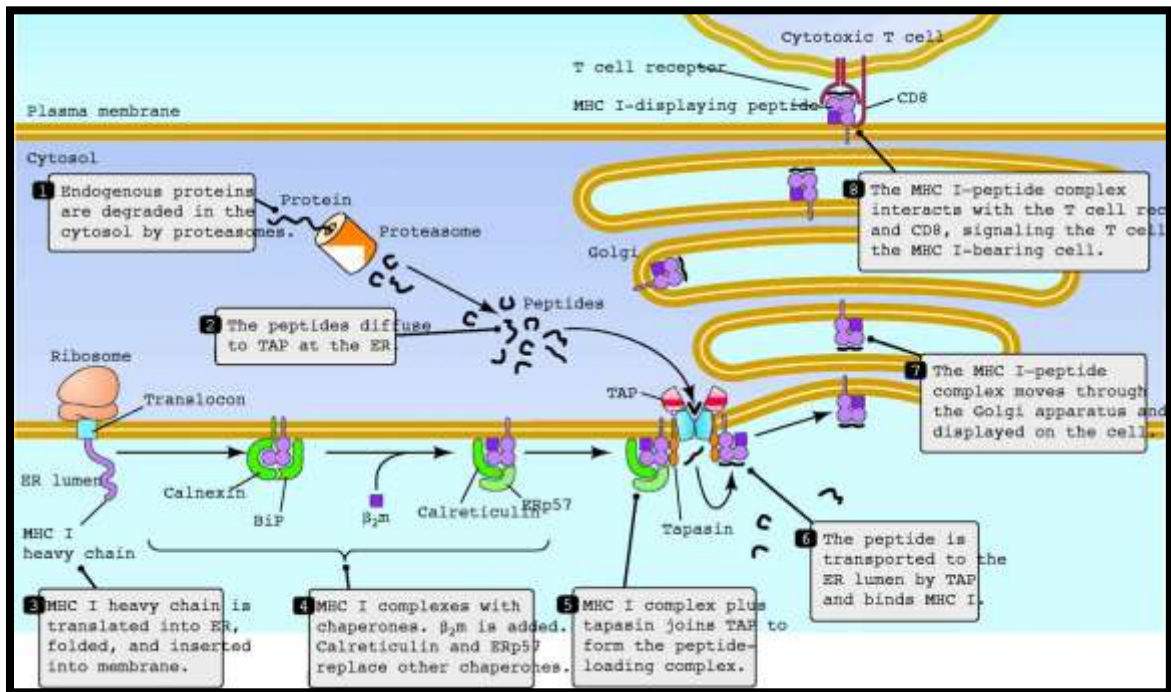


Figure 3: Overview of the MHC I antigen-processing pathway- TAP (Transporter Associated with antigen Processing), ER (Endoplasmic Reticulum), MHC I (Major Histocompatibility Complex), BiP (Immunoglobulin Binding Protein), β_2m , β_2 -microglobulin (Adapted from Rupert and Robert 2004).

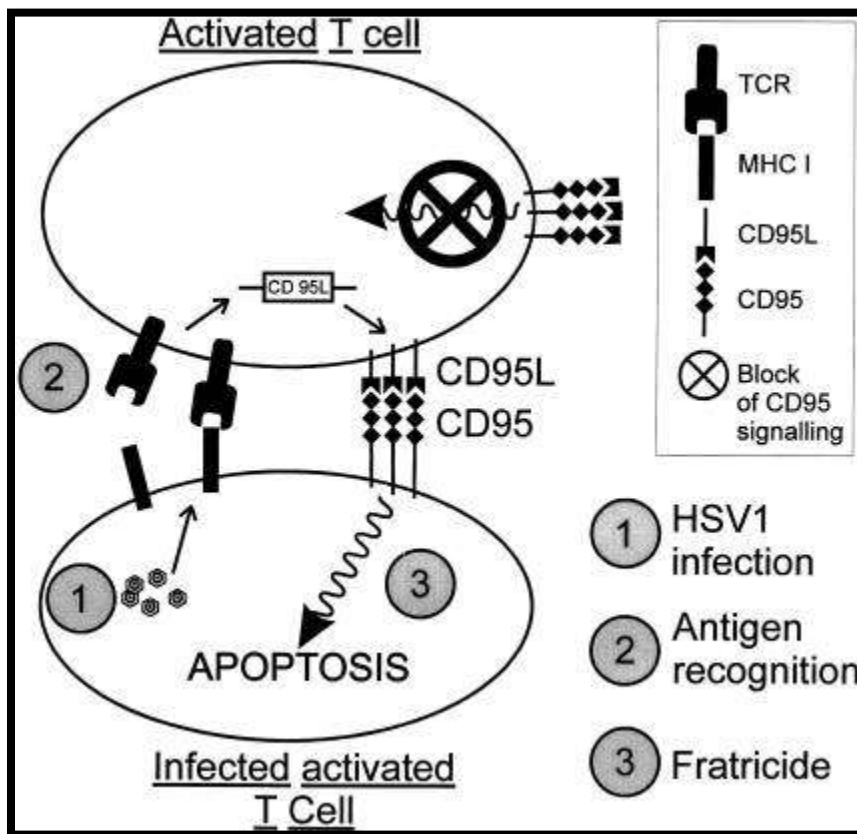


Figure 4: HSV1-induced fratricide of antiviral CTLs as a mechanism of viral immune evasion. Antiviral CTLs activated in the draining lymph nodes enter the epithelial lesions, where they are infected by HSV1 virions 1. Due to inefficient activity of the TAP (Transporter Associated with antigen Processing) blocker in T lymphocytes, viral antigens are presented via the MHC class I molecules and recognized by neighboring CTLs 2. In addition, HSV1 lifts the block for CD95-mediated death signals, resulting in fratricide (Adapted from Raftery et al., 1999).

In the current study IFN- γ was used to rescue the murine fibroblast and keratinocyte cell lines from HSV-1 induced MHC class I down regulation. IFN- γ plays a major antiviral role during HSV1 infection. It was observed that IFN- γ produced by CD8⁺ T cells is effective against HSV-1 infection in adaptive immunity. IFN- γ signaling

begins with interaction of IFN- γ with an IFN receptor complex consisting of two IFNGR1 molecules and two IFNGR2 molecules (Waiboci et al., 2007). The C-terminus of IFN- γ consists of a nuclear localization sequence (NLS), which plays an important role in binding of IFN- γ to IFNGRs. Endocytosis of IFN- γ into the cell occurs with an interaction of IFN- γ NLS domain to IFNGR1. This induces JAK2 auto phosphorylation on tyrosine residues. Auto phosphorylation of JAK2 induces activation and phosphorylation of STAT1, then STAT1 delivers a signal to the nucleus. IFNs (type I and II) select their specific pair of Janus Kinase (JAK), signal transduction and transcription (STAT) group for translocation of signal to the nucleus (Yokota et al., 2005). In case of HSV-1 infection, IFN- γ in the trigeminal ganglia plays a key role in controlling the infection by inhibition of reactivation and inhibition of ICP0 (Minami et al., 2002). SOCS-1 is an inhibitor of JAK which in turn down regulates IFN- γ expression in keratinocytes (Frey et al., 2009).

SOCS (Suppressor of Cytokine Signaling) proteins are a family of 8 members; SOCS-1, SOCS-2, SOCS-3, SOCS-4, SOCS-5, SOCS-6, SOCS-7 and cytokine-inducible SH2 protein. SOCS has a kinase inhibitory region (KIR) and SRC Homology 2 (SH2) domains that plays an important role in binding of SOCS-1 to JAK2. When the KIR region binds to JAK2 tyrosine residue, inhibits the autophosphorylation of STAT1a. Inhibition of STAT1a autophosphorylation leads to blockage of the IFN- γ signaling pathway. By the use of SOCS mimetic or Tyrosine kinase inhibitory peptide (Tkip) during HSV-1 infection, it was observed that peptide mimetic is attached to tyrosine residue of JAK2. This stops STAT1a phosphorylation during IFN- γ signaling. SOCS-1

peptide antagonist binds to the KIR region of SOCS-1 that allows JAK2 phosphorylation, STAT1a phosphorylation and IFN- γ signaling pathway continues (Waiboci et al., 2007).

Viruses have developed successful strategies to overcome the protective effects of interferons (Peng et al, 2008). HSV-1 infection can induce strong cytokine response in infected cells such as type I interferons (IFN- α & IFN- β). In keratinocytes HSV-1 infection induces large amounts of IFNs as well as interleukins (IL) 1, 6, and chemokines (Sprecher et al., 1992). In Human epidermal keratinocytes, INF- γ pretreatment induced HLA-DR expression and protected the cells from HSV-1 induced MHC class I down regulation (Mikloska et al., 1996). Antiviral effects of IFN- γ and IFN- γ peptide mimetic protected fibroblast (L929) cells from HSV-1 induced cytopathic effect, whereas keratinocyte (HEL-30) cell lines derived from C3H mice were not protected during the studies. Identical results were observed with cell lines PAM-212 and A2R1. PAM-212 keratinocytes were not protected by IFN- γ during HSV-1 infection and A2R1 fibroblasts were protected through antiviral effect of the IFN- γ (Frey et al., 2009).

CD8⁺ T-cells control HSV-1 infection by exocytosis of lytic granules or by secretion of cytokines IFN- γ and TNF- α (Sheridan et al., 2007). CD8⁺ T-cells also control the maintenance of latency and prevent reactivation of HSV-1. In ex-vivo cultures of latently infected ganglia, IFN- γ and granzyme B secreted by CD8⁺ T cells inhibited HSV-1 reactivation by degrading the ICP4 protein (crucial for lytic events) (Knickelbein et al., 2008). HSV-1 interferes with presentation of antigen on MHC class I molecules (Lacaille and Androlewicz, 1998), in such situation CTL responses would be insufficient for viral clearance. Since IFN- γ can up regulate MHC I expression (Mikloska et al., 1996), this is critical in controlling HSV-1.

The hypothesis of this study is HSV-1 infection of murine fibroblasts and keratinocytes inhibits expression of MHC class I molecules during first 24 hours of infection. IFN- γ pretreatment of fibroblasts protected them from virus-induced inhibition of MHC class I expression, but did not protect keratinocytes.

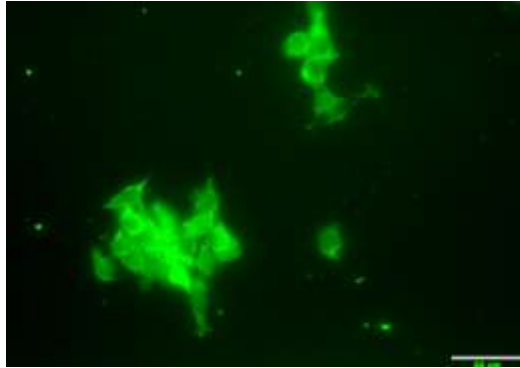
In the current study, fibroblast and keratinocyte cell lines derived from C3H mice (L929 fibroblasts and HEL-30 keratinocytes) and BALB/c mice (A2R1 fibroblasts and PAM-212 keratinocytes) responded differently to IFN- γ induction of MHC class I expression in HSV-1 infected and IFN- γ pretreated cells. L929 and A2R1 cells expressed higher levels of MHC class I when treated with IFN- γ than keratinocytes. Different MOI's were used to determine the appropriate dilution to use on the cell lines. 0.1 MOI was chosen because it has cytopathic effects on the cells. Frey et al., observed loss of cell viability (keratinocytes and fibroblasts) when infected for 48 hours with HSV-1 at 0.1 MOI (Frey et al., 2009). It would be appropriate to observe for the MHC class I expression up to 24 hours post infection, since the cell viability will be lost by 48 hours post infection.

The C3H mouse was partially resistant to infection by HSV-1 (Armerding and Rossiter, 1981). Type I IFN production has been proposed as a mechanism for resistance (Chmielarczyk et al., 1985). High levels of Type I IFNs were seen in exudates as soon as 2-4 hours after infection (Engler et al., 1982). In contrast, BALB/c mice were not known to be resistant and they produce low levels of Type I IFNs (Watanabe et al., 1999). These two mouse cell lines were selected for the current study to identify if the IFN- γ pretreatment of control cells and infected cells leads to any variation in their resistance

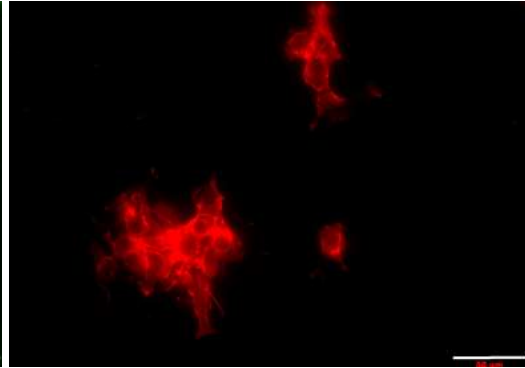
pattern. Frey et al., observed that higher concentration of IFN- γ showed more protection for HSV-1 infection in fibroblast cell lines when compared using lower concentration of IFN- γ (Frey et al., 2009). Based on their data, a higher concentration of IFN- γ (100 units/ml) has been used in this study.

Immunofluorescence staining was performed for murine fibroblast cell lines (L929 and A2R1) at 6, 12, and 24 hours intervals post infection with HSV-1, to compare MHC class I expression. Image J software developed by NIH (National Institute of Health) was used for analyzing the images of MHC class I stained L929 and A2R1 cells. Images of the cells stained for actin and MHC class I were merged through Image J software. Flow cytometry technique was performed for all four cell lines (fibroblasts and keratinocytes) after 24 hours of infection. The reason for choosing 24 hours post infection time point was that immunocytochemistry results exhibited high MHC class I expression for IFN- γ pretreatment, and MHC class I expression was significantly decreased during HSV-1 infection, when compared to 6 and 12 hours post infection time point. However, for keratinocytes (HEL-30 (Figure 5), and PAM-212) immunolocalization was not possible because cells grew in clusters and the staining patterns in individual cells could not be analyzed by Image J software. Immunofluorescence staining performed for keratinocytes HEL-30 (Figure 5) showed an unclear staining pattern. For better results the immunofluorescence staining for HEL-30 cells was repeated by trypsinizing the cells to separate them from clumping, resulting in less cell density and decrease in immunofluorescence intensity due to the loss of cells and disruption of cell membranes (Figure 6). Hence it was concluded that this method was not appropriate and flow cytometry technique was selected for identifying MHC class I expression.

(a) MHC class I stained



(b) Actin stained



(c) Merged

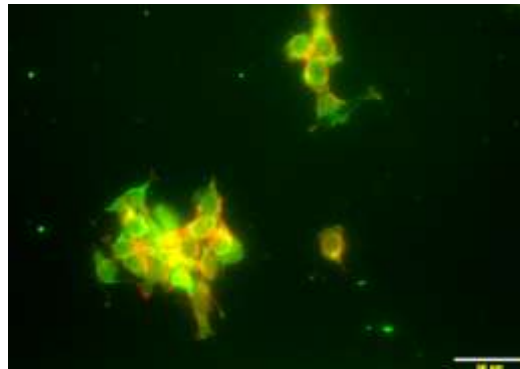
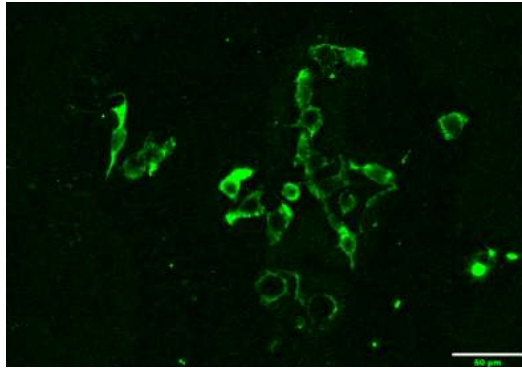
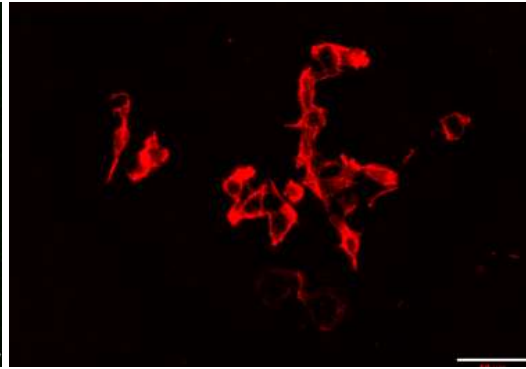


Figure 5: Images of HEL-30 cells treated with antibodies for (a) MHC class I (green), (b) actin (red), and (c) MHC class I and actin merged. Bar marker indicate 50 μm size.

(a) MHC class I stained



(b) Actin stained



(c) Merged

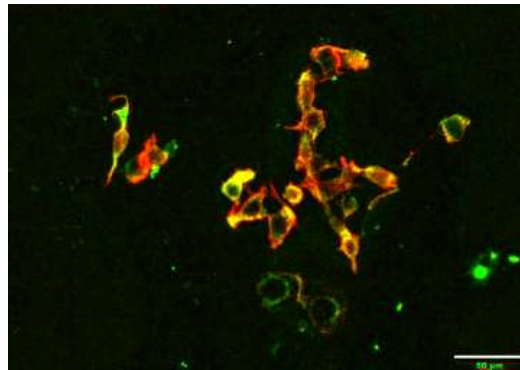


Figure 6: Images of trypsinized HEL-30 cells treated with antibodies for (a) MHC class I (green), (b) actin (red), and (c) MHC class I and actin merged. Bar marker indicate 50 μm size.

MATERIALS AND METHODS

Cell Culture:

L929 cells from C3H mice and A2R1 cells of BALB/C mice are fibroblasts that populate the dermal layer of the skin. HEL-30 keratinocytes derived from C3H mice, (Dr. Janice Speshock, Wright Patterson Air Force Base), PAM-212 keratinocytes derived from BALB/c mice (American Type Culture Collection) and Vero cells (CCL-81, ATCC) were cultured in Dulbecco's Modified Eagles Medium (DMEM) (Fisher Scientific, catalog # SH30243.01) supplemented with 10% heat-inactivated fetal calf serum, and 1µl/ml gentamicin solution. The cells were grown on 100 mm² tissue culture dishes and incubated in a humidified incubator at 37° C with 5% CO₂.

Virus:

Herpes Simplex Virus-1 strain Syn 17+ (Dr.Nancy Sawtell, Children's Hospital Medical Center, Cincinnati, OH) was propagated in the lab. Vero cells were grown in a 75cm² flask and a confluent monolayer was infected with HSV-1 at 0.1 multiplicity of infection (MOI). Cells were examined and harvested along with medium when cytopathic effects (cells rounding and detaching from the bottom of the flask) were evident after 3-5 days of infection. Medium was stored as virus stock in 100 µl aliquots at -80°C. The number of plaque forming units (PFU) were calculated after performing a plaque assay on Vero cells. The virus was dispensed at 0.1 MOI in DMEM containing 2% calf serum on the cell monolayer in the 24 well culture plates, and then placed in an incubator at 37°

C. The virus was left on the cells for 2 hours and then the culture medium was removed and replaced with fresh culture medium. Mock infected cells were treated in the same way, except 2% DMEM was used instead of 10% DMEM. For immunostaining, each cell line was added to sterile glass coverslips that were placed in 24 well plates and infected as previously described.

IFN- γ pretreatment and virus infection of cells for immunocytochemistry:

L929 and A2R1 cells were treated with IFN- γ (Peprotech, catalog # 315-05) at concentration of 100 units/ ml for 24 hours and then infected with HSV-1 at 0.1 MOI. A list of treated groups and infected groups were detailed in Table 1.

Cell group treated	IFN-γ	HSV-1
Cell only	-	-
Cell+ virus	-	+
Cell+ IFN- γ	+	-
Cell+ IFN- γ + virus	+	+

Table 1: List of treated cell groups for current study, specifying which groups are treated with IFN- γ and infected with HSV-1.

Immunocytochemistry for MHC class I antigen and actin:

At the end of 6, 12, and 24 hours post infection time points, immunocytochemistry was performed.

Immunocytochemistry procedure for L929 and HEL-30 cells:

- 1) The cells were rinsed once with phosphate buffered saline (PBS), at room temperature (RT) and then the PBS was removed.
- 2) 4% paraformaldehyde fixative (to preserve cell morphology) was added, and the cells were incubated at RT for 15 minutes.
- 3) The paraformaldehyde fixative was removed, and quenched with sodium borohydride (1mg/ml) that was prepared just prior to use. The cells were incubated in this solution for 15 minutes at RT.
- 4) The cells were then washed 3 times with PBS.
- 5) 3% BSA (Bovine Serum Albumin) blocking solution was added to the cells and incubated at RT for 30 minutes.
- 6) The primary biotin conjugated anti mouse MHC I (H-2Kk) (ebiosciences, catalog # 13-5940-82) was prepared in the blocking buffer (diluted 1:100) and then it was applied to each coverslip.
- 7) The coverslips were placed in a humidified chamber cell side down, and allowed to incubate at 4° C overnight.
- 8) Then coverslips were transferred back to their dishes, and washed three times with PBS.
- 9) The secondary FITC conjugated streptavidin (ebiosciences, catalog # 11-4317-87) prepared in the blocking buffer (diluted 1:100) and Texas red conjugated phalloidin (Life technologies, catalog # T7471) for actin staining was prepared in the same blocking buffer (diluted 1:100) were applied to each coverslip, and allowed to incubate for 2 hours at RT in the dark.

- 10) The coverslips were placed back into their dishes, and washed 3 times with PBS.
- 11) The coverslips were mounted onto glass slides using liquid mounting medium-Vectashield (Vector Labs), and sealed with clear nail varnish.

Immunocytochemistry procedure for A2R1 and PAM 212 cells:

- 1) The cells were rinsed once with phosphate buffered saline (PBS), at room temperature (RT) and then the PBS was removed.
- 2) 4% paraformaldehyde fixative was added, and the cells were incubated at RT for 15 minutes.
- 3) The paraformaldehyde fixative was removed, and quenched with sodium borohydride (1mg/ml) that was prepared just prior to use. The cells were incubated in this solution for 15 minutes at RT.
- 4) The cells were then washed 3 times with PBS.
- 5) 3% BSA blocking solution was added to the cells which were incubated at RT for 30 minutes.
- 6) Direct FITC conjugated anti mouse MHC I (H-2Kd/H-2Dd) (ebiosciences, catalog # 11-5998-82) was prepared in the blocking buffer (diluted 1:100) and Texas red conjugated phalloidin (Life technologies, catalog # T7471) for actin staining was prepared in the same blocking buffer (diluted 1: 100). Each antibody was applied to each coverslip, and allowed to incubate for 2 hours at RT in the dark.
- 7) The coverslips were placed back into their dishes, and washed 3 times with PBS.
- 8) The coverslips were mounted onto glass slides using liquid mounting medium-Vectashield (Vector Labs), and sealed with clear nail varnish.

Cells were observed under fluorescent microscope (Olympus Epi Fluorescence Spot Scope with real time color camera) and two images were taken per field. Two different filters (filter # 4 and 5) were used to capture images for one field, because each secondary antibody used has a different fluorescent label. Three fields were observed for each group per experiment, and three experiments were performed at each of the time points identified.

Image J software by NIH (National Institute of Health) was used to measure MHC class I fluorescence intensity of L929 and A2R1 immunostained images. The pixel intensity was measured, and the mean fluorescent intensity was calculated using Image J software. At least three fields per group, and a minimum of three experiments were performed. A list of antibodies and isotype controls that were used are detailed in Table 2.

Antibodies type	L929 cells	A2R1 cells	HEL 30 cells	PAM 212 cells
Primary (MHC class I)	biotin conjugated anti mouse MHC I (H-2Kk) (ebiosciences, catalog # 13-5940-82)	FITC conjugated anti-mouse MHC I (H-2Kd/H-2Dd) (ebiosciences, catalog # 11-5998-82)	biotin conjugated anti mouse MHC I (H-2Kk) (ebiosciences, catalog # 13-5940-82)	FITC conjugated anti-mouse MHC I (H-2Kd/H-2Dd) (ebiosciences, catalog # 11-5998-82)
Secondary (MHC class I)	FITC conjugated streptavidin (ebiosciences, catalog # 11-4317-87)		FITC conjugated streptavidin (ebiosciences, catalog # 11-4317-87)	
Actin	Texas red conjugated phalloidin (Life technologies, catalog # T7471)	Texas red conjugated phalloidin (Life technologies, catalog # T7471)	Texas red conjugated phalloidin (Life technologies, catalog # T7471)	Texas red conjugated phalloidin (Life technologies, catalog # T7471)
Isotype control	biotin conjugated mouse IgG1 (ebiosciences, catalog # 13-4714-85)	FITC conjugated mouse IgG2a (ebiosciences, catalog # 11-4724-82)	biotin conjugated mouse IgG1 (ebiosciences, catalog # 13-4714-85)	FITC conjugated mouse IgG2a (ebiosciences, catalog # 11-4724-82)

Table 2: List of antibodies and isotype controls used to stain cells for immunocytochemistry and flow cytometry.

Flow Cytometry:

Cells were harvested for flow cytometry at the 24 hours post infection time point and cells were detached from the plate with cell stripper solution (Cell grow, catalog #

25-056-CI). After assessing cell count and viability by trypan blue exclusion, 10^6 cells per sample were transferred to 2 ml vial.

Flow cytometry procedure for L929 and HEL-30 cells:

- 1) To perform surface staining, samples were washed twice with 1% BSA, and blocked for 1 hour with 3% BSA.
- 2) L929 and HEL 30 cells were stained with biotin conjugated anti mouse MHC I (H-2Kk) (ebiosciences, catalog # 13-5940-82) that was prepared in the blocking buffer (diluted 1:100) and incubated for 1 hour at 4°C.
- 3) Samples were washed twice with 1% BSA and stained with FITC conjugated streptavidin (ebiosciences, catalog # 11-4317-87) that was prepared in the blocking buffer (diluted 1:100) and incubated for 1 hour at 4°C.
- 4) After incubation the samples were washed twice with 1% BSA.
- 5) The final pellet was suspended in 1% sodium azide solution.

Flow cytometry procedure for L929 and A2R1 and PAM-212 cells:

- 1) L929 and HEL 30 cell samples were washed twice with 1% BSA, and blocked for 1 hour with 3% BSA.
- 2) Cells were stained with FITC conjugated anti mouse MHC I (H-2Kd/H-2Dd) (ebiosciences, catalog # 11-5998-82), that was prepared in the blocking buffer (diluted 1:100) and incubated for 1 hour at 4°C.
- 3) After incubation the samples were washed twice with 1% BSA.
- 4) The final pellet was suspended in 1% sodium azide solution.

For all the samples, flow cytometry was performed using C6 flow cytometer (BD Accuri), and analyzed with FCS Express 4 plus research edition.

Statistical Analysis:

Using Sigma Plot 12.0, statistical analysis was performed for the Image J analyzed fluorescence intensity values and mean fluorescence intensity values of flow cytometry. The values expressed are the Standard Error of the Mean (SEM). The Holm-Sidak method was used to determine the significance between the treated groups and the control groups.

RESULTS

Immunocytochemistry for L929 fibroblast cells:

HSV-1-infected L929 fibroblasts exhibited a decrease in MHC class I fluorescence intensity at 6 hours post infection (Figure 7) compared with untreated cells. When these cells were pretreated with IFN- γ , there was an increase in MHC class I expression in both infected and uninfected cells.

After 12 hours of infection (Figure 8) there was a significant decrease in MHC class I fluorescence intensity in the virus infected cells, when compared with untreated cells. When these cells were pretreated, there was an increase in the MHC class I expression in both infected and uninfected cells. A decrease in cell density was observed in the HSV-1 infected group.

After 24 hours of infection (Figure 8 & 10c), there was a significant decrease in MHC class I fluorescence intensity in the virus infected cells when compared with untreated cells. When these cells were pretreated with IFN- γ , there was an increase in the MHC class I expression both in infected and uninfected cells. During HSV-1 infection there was a decrease in the density of cells (Figure 9b & 9d).

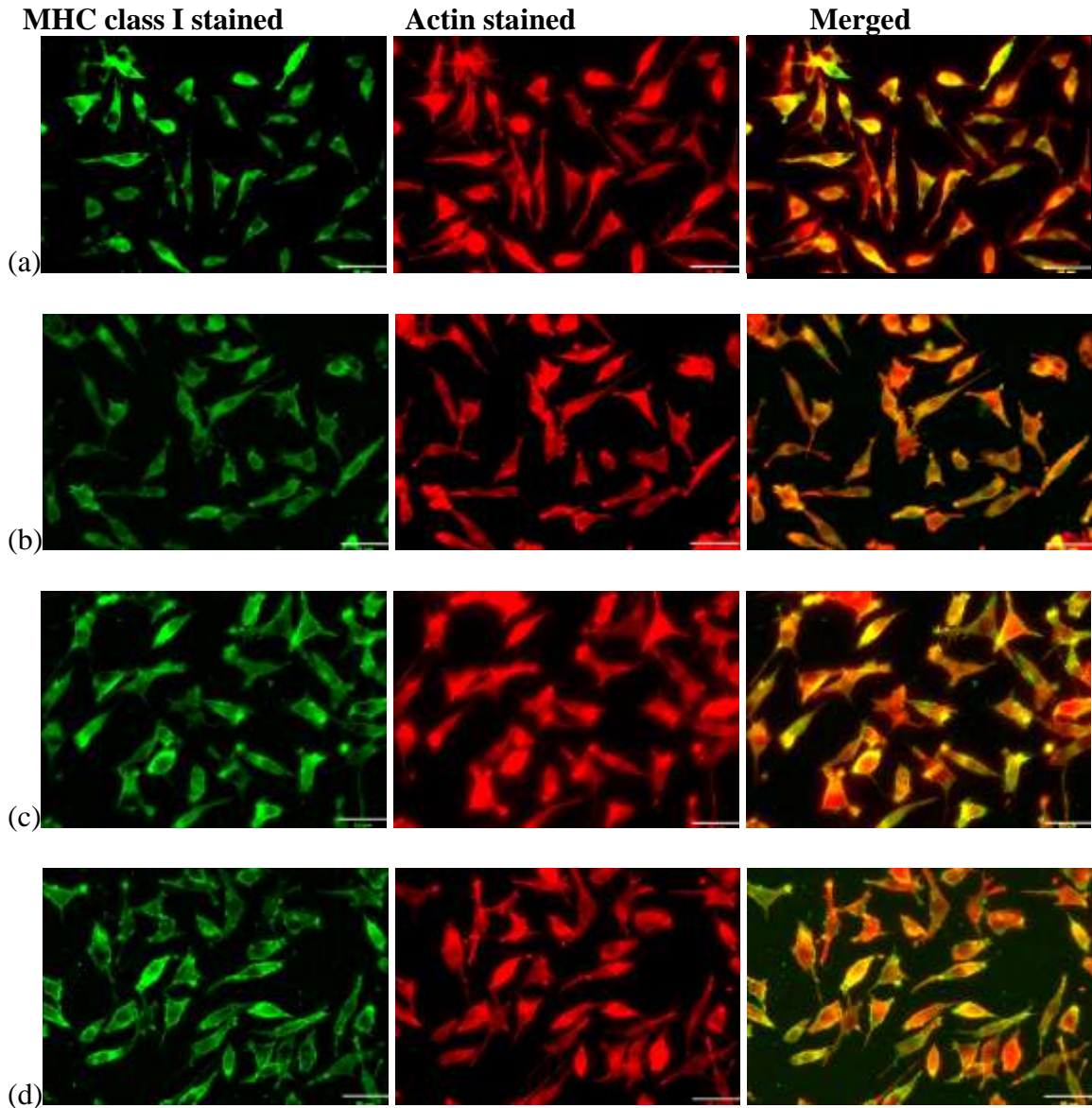


Figure 7: Immunocytochemistry for L929- 6 hours post infection MHC class I stained(Green) and actin stained(Red) images: HSV-1 control (a), L929+HSV-1, (b) L929+ IFN- γ (c), L929+ IFN- γ + HSV-1(d). At 6 hours post infection, no difference in cell density was observed in between L929 uninfected cells and cells infected with HSV-1 virus. IFN- γ pretreated cells showed more fluorescent intensity when compared to cells only. Bar markers indicate 50 μ m.

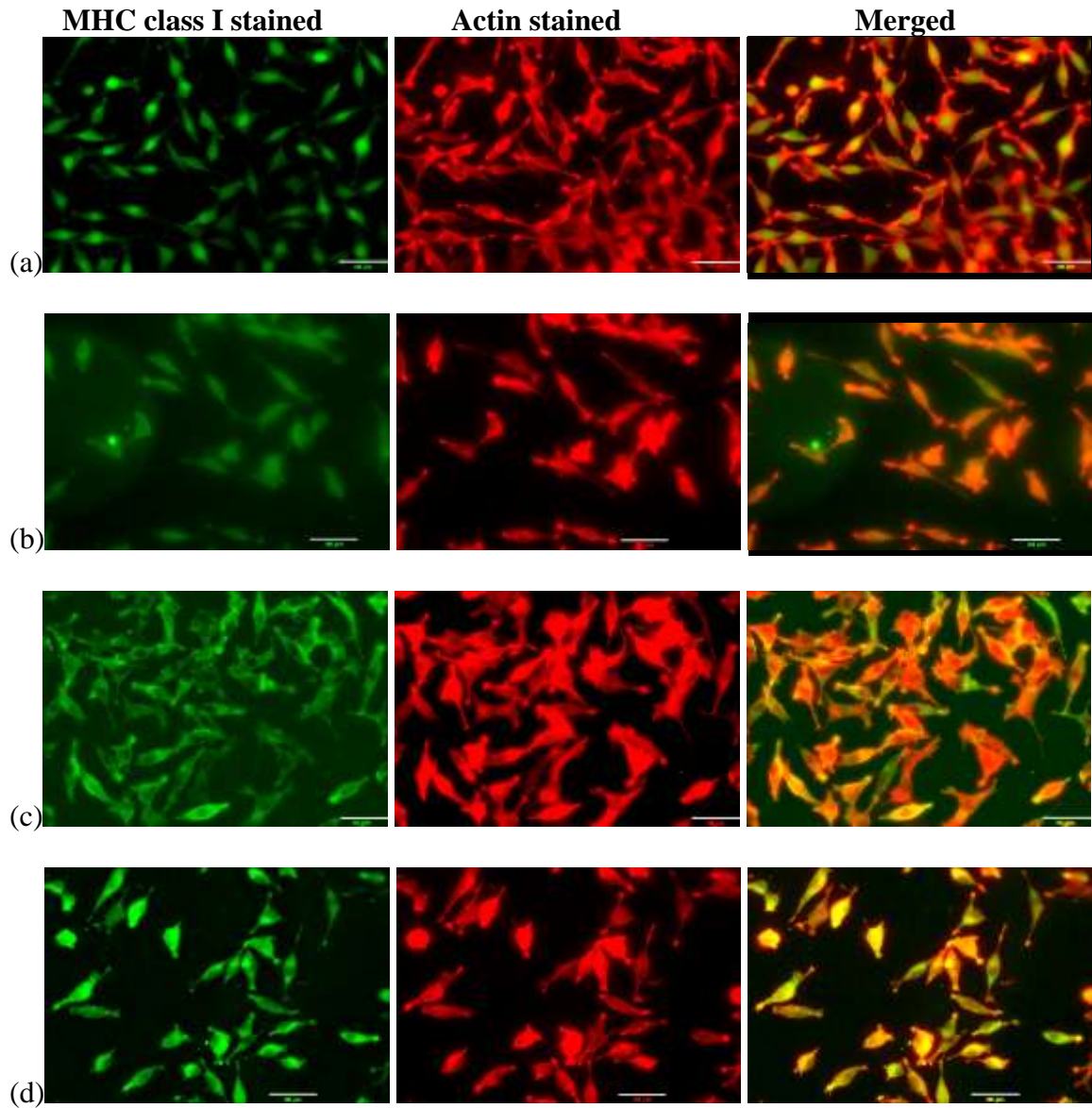


Figure 8: Immunocytochemistry for L929- 12 hours post infection MHC class I stained (Green) and actin stained (Red) images: HSV-1 control (a), L929+HSV-1, (b) L929+ IFN- γ (c), L929+ IFN- γ + HSV-1 (d). At 12 hours post infection, a decrease in cell density was observed in infected group when compared with uninfected group. IFN- γ pretreated and HSV-1 infected cells showed more fluorescent intensity when compared to infected cells. Bar markers indicate 50 μ m.

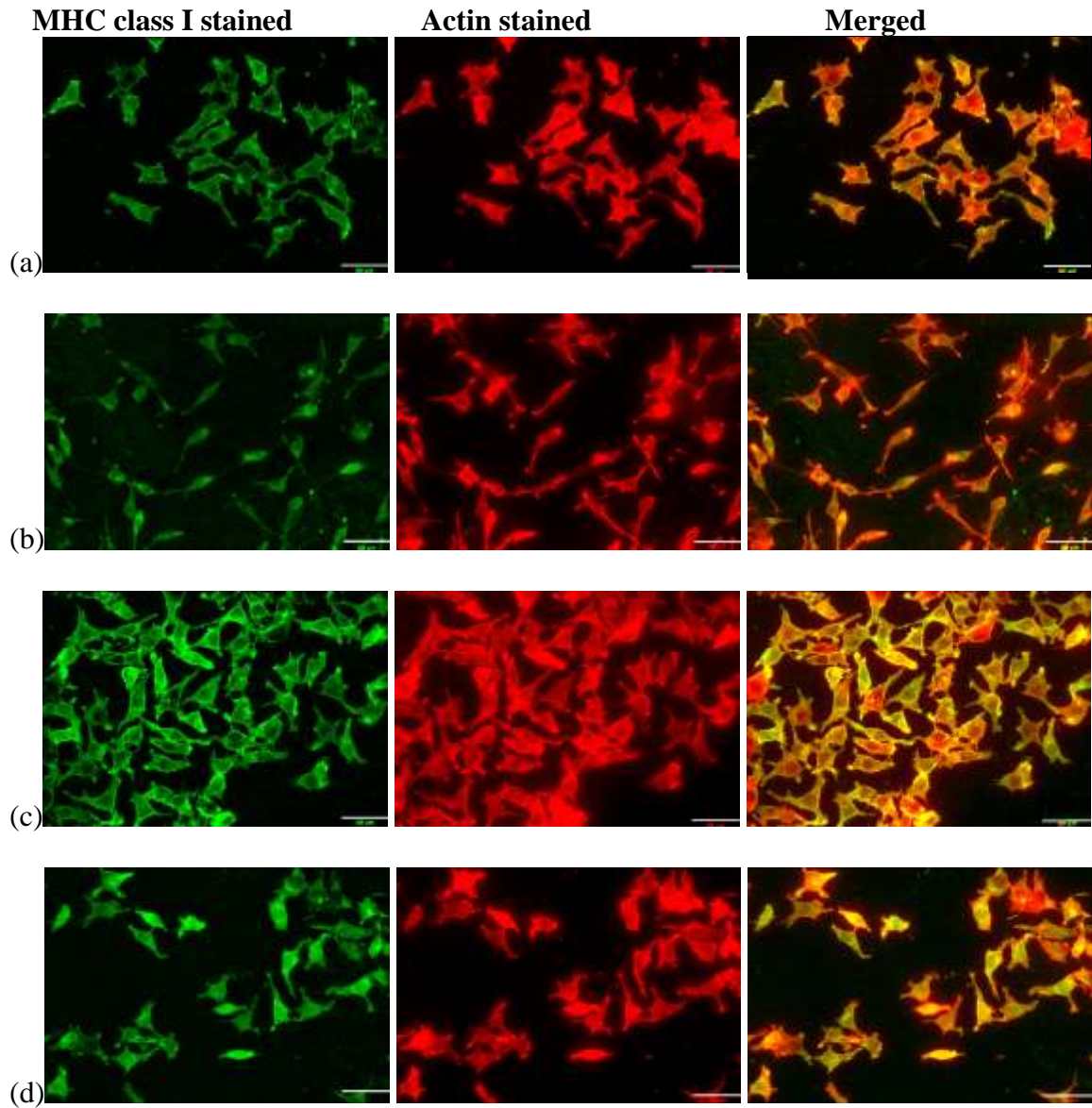


Figure 9: Immunocytochemistry for L929- 24 hours post infection MHC class I stained(Green) and actin stained(Red) images: HSV-1 control (a), L929+HSV-1, (b) L929+ IFN- γ (c), L929+ IFN- γ + HSV-1 (d). At 24 hours post infection, a decrease in cell density was observed in infected group when compared with uninfected group. IFN- γ pretreated and HSV-1 infected cells showed more fluorescent intensity when compared to infected cells. Bar markers indicate 50 μ m.

Image J quantification of MHC class I fluorescence intensity for L929 fibroblasts :

When the mean fluorescence was measured and compared, there was a significant increase in the IFN- γ treated cells when compared with untreated cells (Figure 10).

After 6, 12, and 24 hours of infection (Figure 10), the virus-infected cells showed a significant decrease in the immunofluorescence intensity, compared to control cells.

After 24 hours of infection (Figure 10c), there was a significant decrease in immunofluorescence intensity both with virus infected, and uninfected cells. At 24 hours post infection, the IFN- γ pretreated expressed one fold increase in immunofluorescence intensity, compared with untreated cells. An increase in MHC class I fluorescence intensity was observed in IFN- γ pretreated, and HSV-1 infected L929 fibroblast cells, compared with control cells (Figure 10).

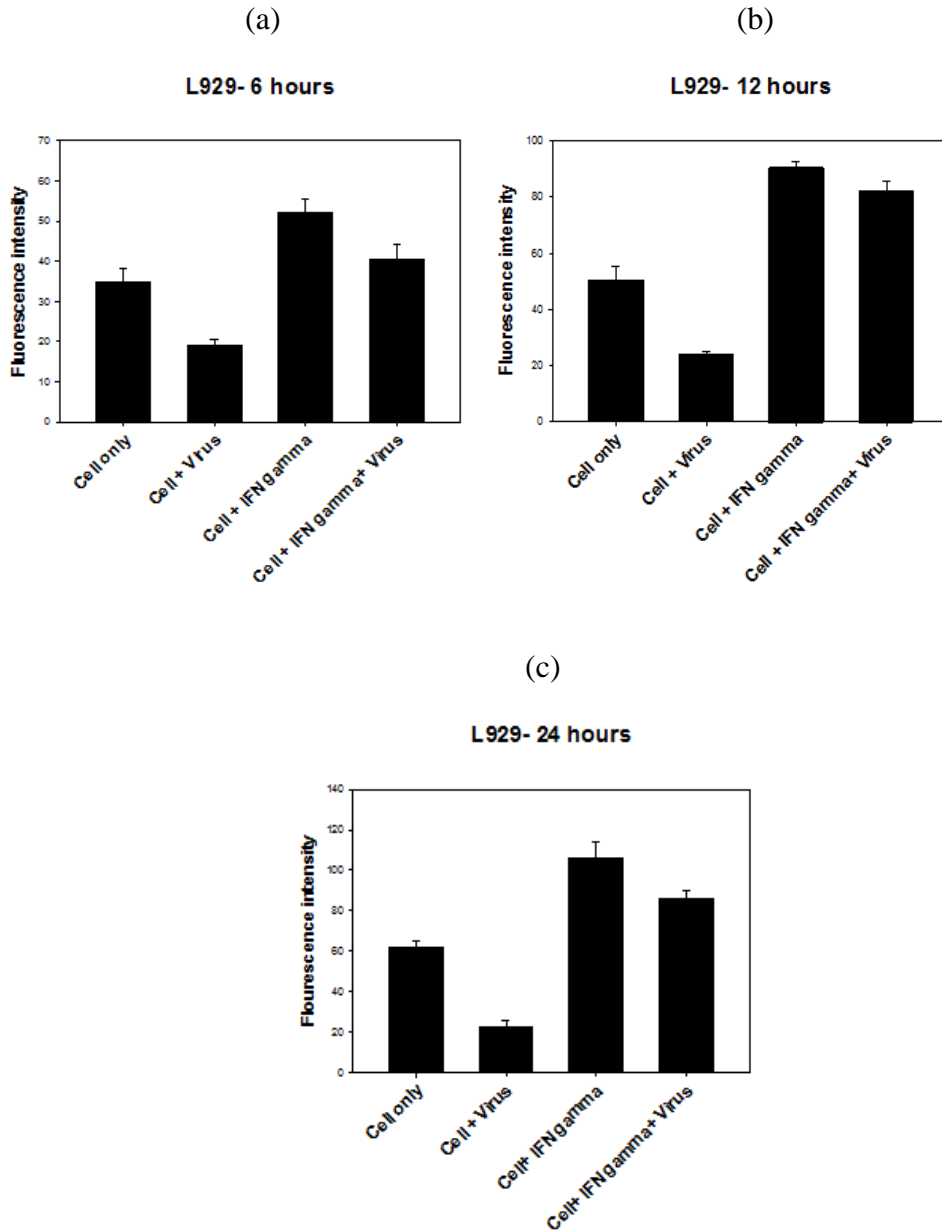


Figure 10: MHC class I fluorescent Intensity using image J program for L929 fibroblasts at 6, 12, and 24 hours post infection. L929 fibroblasts at 6 hours post infection (a), L929 fibroblasts at 12 hours post infection (b), L929 fibroblasts at 24 hours post infection (c). At 6, 12 and 24 hours post infection, the MHC class I fluorescence intensity increased significantly ($P < 0.001$ by ANOVA) in the cells pretreated with IFN- γ and infected with HSV-1 when compared with the infected cells.

Immunocytochemistry for A2R1 fibroblast cells:

HSV-1 infected L929 fibroblasts displayed a decrease in MHC class I fluorescence intensity at 6 hours post infection (Figure 11) compared with untreated cells. When these cells were pretreated with IFN- γ there was an increase in MHC class I expression in both infected and uninfected cell.

After 12 hours of infection (Figure 12), IFN- γ pretreated cells showed an increase in the MHC class I expression both in infected and uninfected cells.

After 24 hours of infection (Figure 13) there was a significant difference between the virus infected cells and the untreated cells. When these cells are pretreated with IFN- γ , there was an increase in the MHC class I both in infected and uninfected cells. During HSV-1 infection there was a decrease in the density of cells (Figure 13b & 13d).

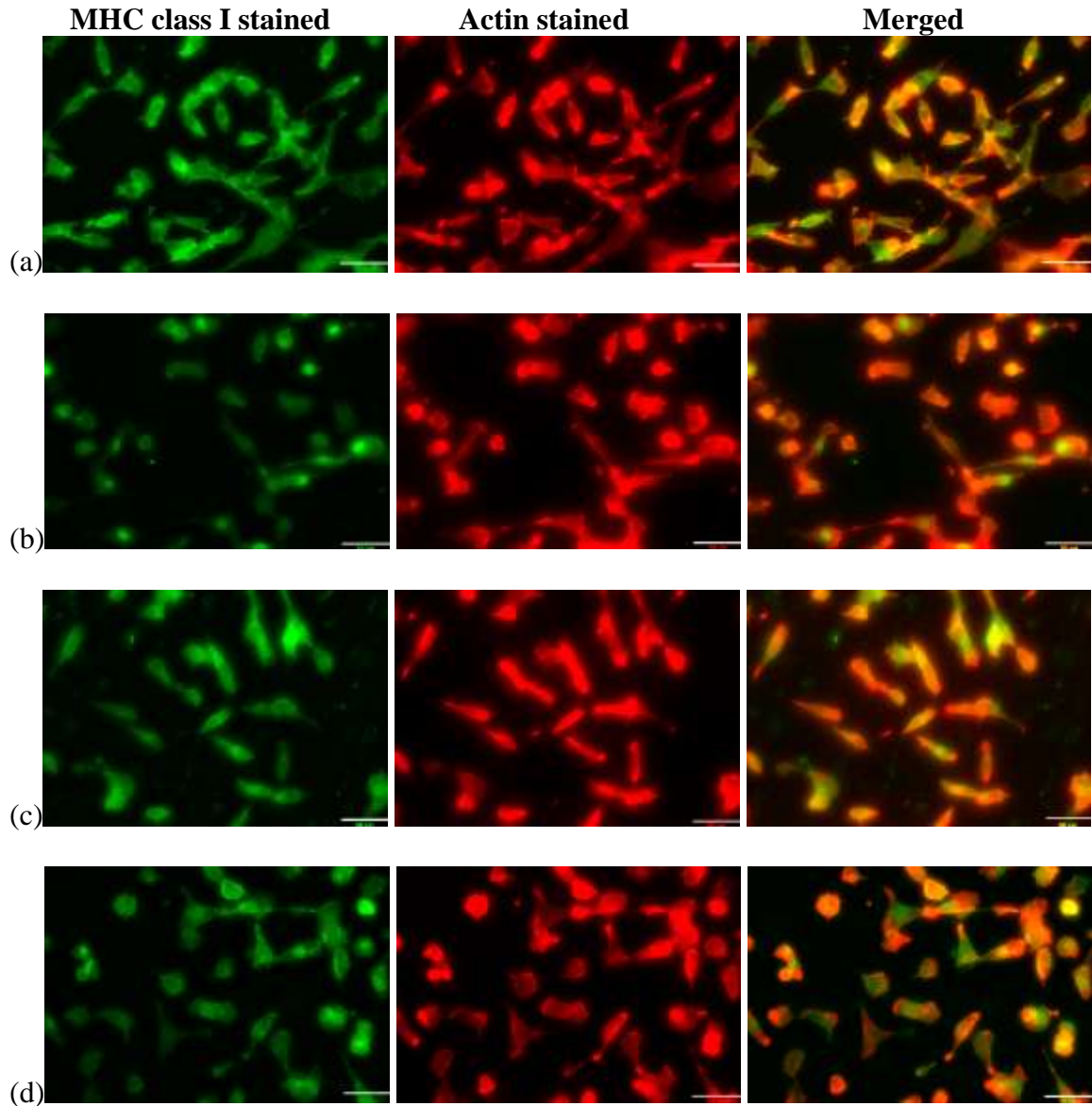


Figure 11: Immunocytochemistry for A2R1- 6 hours post infection MHC class I stained(Green) and actin stained(Red) images: HSV-1 control (a), A2R1+HSV-1, (b) A2R1+ IFN- γ (c), A2R1+ IFN- γ + HSV-1(d). At 6 hours post infection, no difference in cell density was observed in between A2R1 uninfected cells and cells infected with HSV-1 virus. IFN- γ pretreated cells showed more fluorescent intensity when compared with cells only. Bar markers indicate 50 μ m.

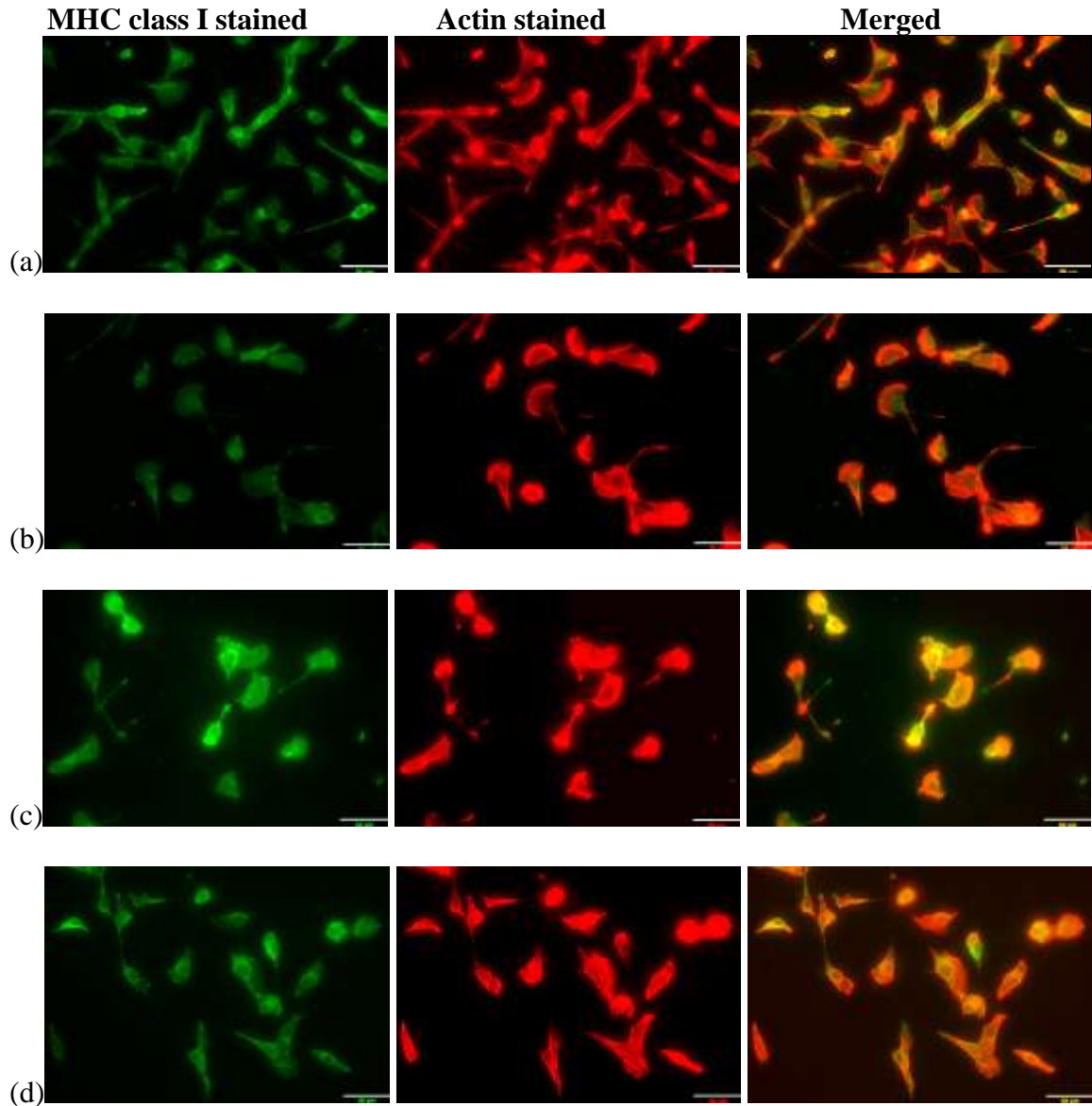


Figure 12: Immunocytochemistry for A2R1- 12 hours post infection MHC class I stained(Green) and actin stained(Red) images: HSV-1 control (a), A2R1+ HSV-1, (b) A2R1+ IFN- γ (c), A2R1+ IFN- γ + HSV-1(d). At 12 hours post infection, a decrease in cell density was observed in infected group when compared to uninfected group. IFN- γ pretreated and HSV-1 infected cells showed more fluorescent intensity when compared with infected cells. Bar markers indicate 50 μ m.

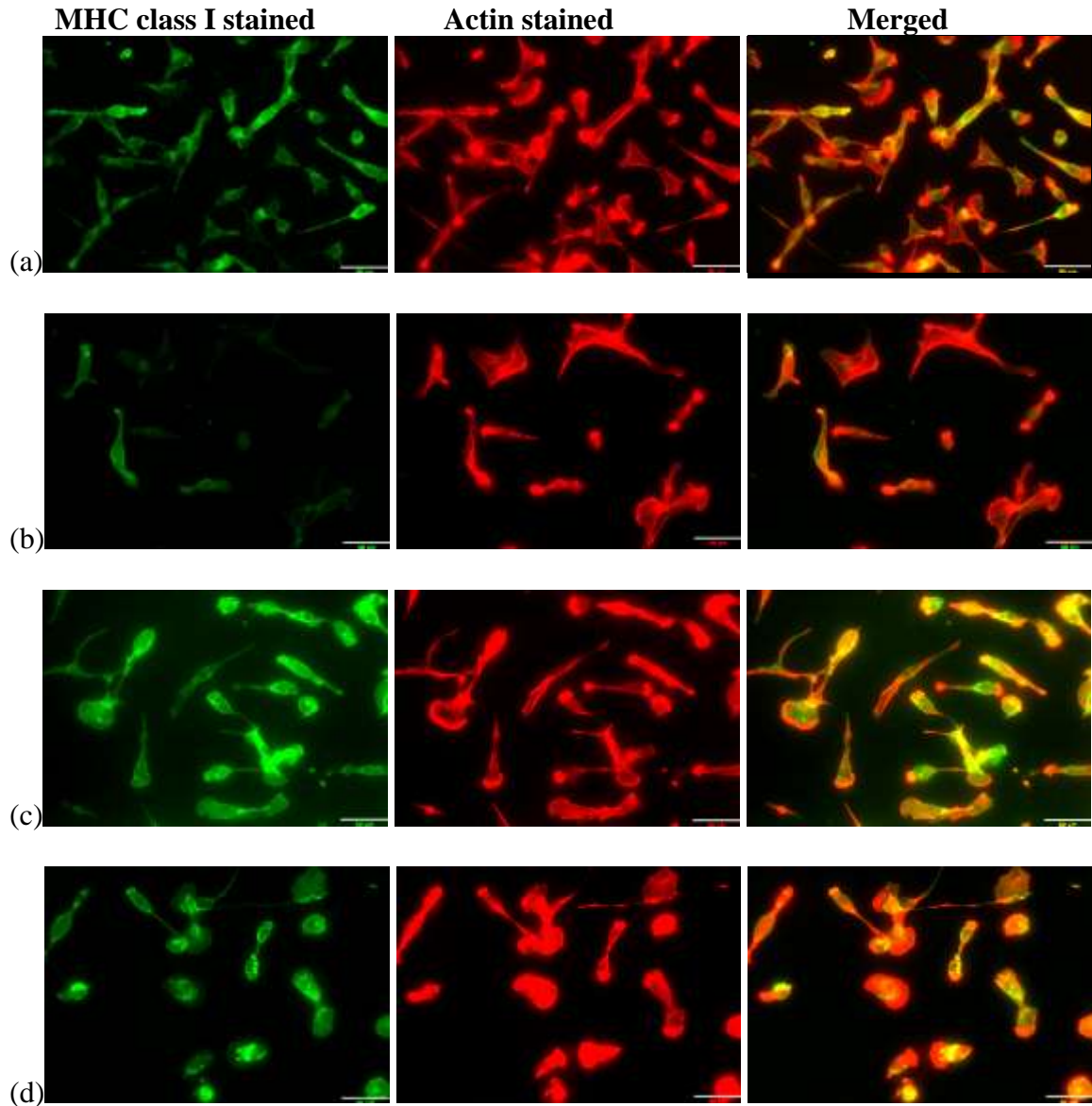


Figure 13: Immunocytochemistry for A2R1- 24 hours post infection MHC class I stained(Green) and actin stained(Red) images: HSV-1 control (a), A2R1+ HSV-1, (b) A2R1+ IFN- γ (c), A2R1+ IFN- γ + HSV-1(d). At 24 hours post infection, a decrease in cell density was observed in infected group when compared to uninfected group. IFN- γ pretreated and HSV-1 infected cells showed more fluorescent intensity when compared with infected cells. Bar markers indicate 50 μ m.

Image J quantification of MHC class I fluorescence intensity for A2R1 fibroblasts :

When the mean fluorescence was measured and compared, there was a significant increase in the IFN- γ treated A2R1 cells compared with untreated cells (figure 14).

After 24 hours of infection (figure 14c), there was a significant decrease in the virus infected and uninfected cells. At 24 hours post infection, the IFN- γ pretreated cells expressed 2 fold increase in immunofluorescence, compared with untreated cells. HSV-1 infected cells with IFN- γ pretreatment exhibited an increase in MHC class I fluorescence intensity, compared to the control cells.

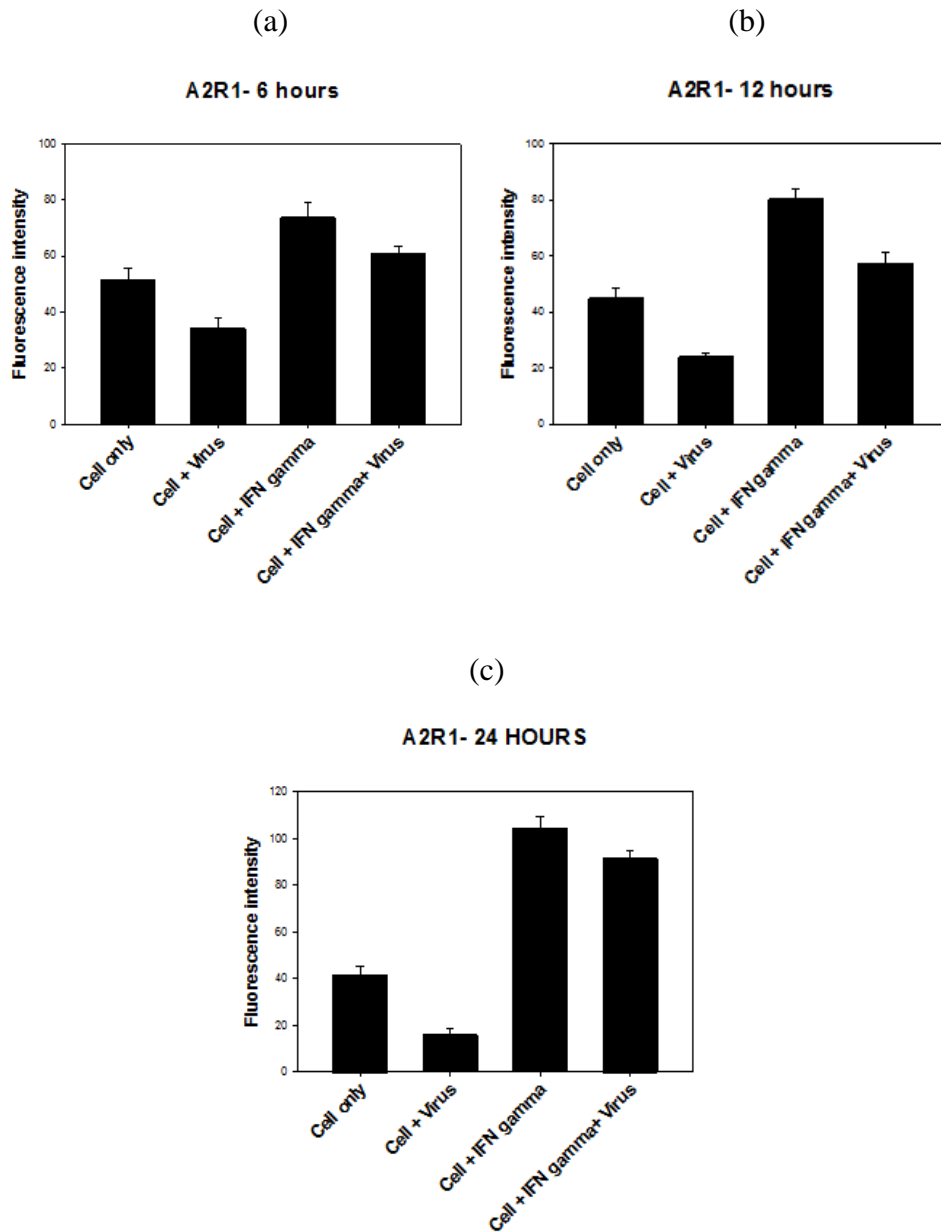


Figure 14: MHC class I fluorescent Intensity using image J program for A2R1 fibroblasts at 6, 12, and 24 hours post infection. A2R1 fibroblasts at 6 hours post infection (a), A2R1 fibroblasts at 12 hours post infection (b), A2R1 fibroblasts at 24 hours post infection (c). At 6, 12 and 24 hours post infection, a significant increase in the MHC class I fluorescence intensity was observed ($P < 0.001$ by ANOVA) in the cells pretreated with IFN- γ and infected with HSV-1 when compared with infected cells.

Comparison of MHC class I fluorescence Intensity for fibroblasts at 6,12 and 24 hours post infection:

For both fibroblast cell lines L929 (Figure 15) and A2R1 (Figure 16), at 6, 12, and 24 hours post infection, a significant increase in the MHC class I fluorescence intensity was observed ($P < 0.001$ by ANOVA) in the cells pretreated with IFN- γ and infected with HSV-1, compared with infected cells.

L929

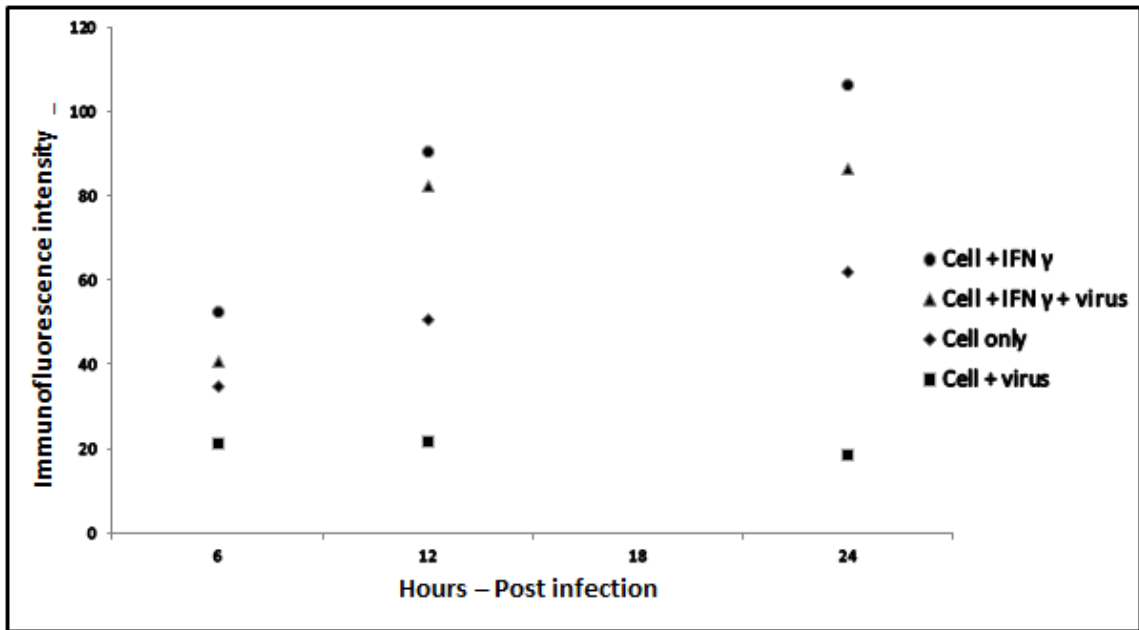


Figure 15: Comparison of MHC class I fluorescent Intensity using image J program for L929 fibroblasts at 6, 12 and 24 hours post infection time points. At 6, 12 and 24 hours post infection, a significant increase in the MHC class I fluorescence intensity was observed ($P < 0.001$ by ANOVA) in the cells pretreated with IFN- γ and infected with HSV-1 when compared to infected cells.

A2R1

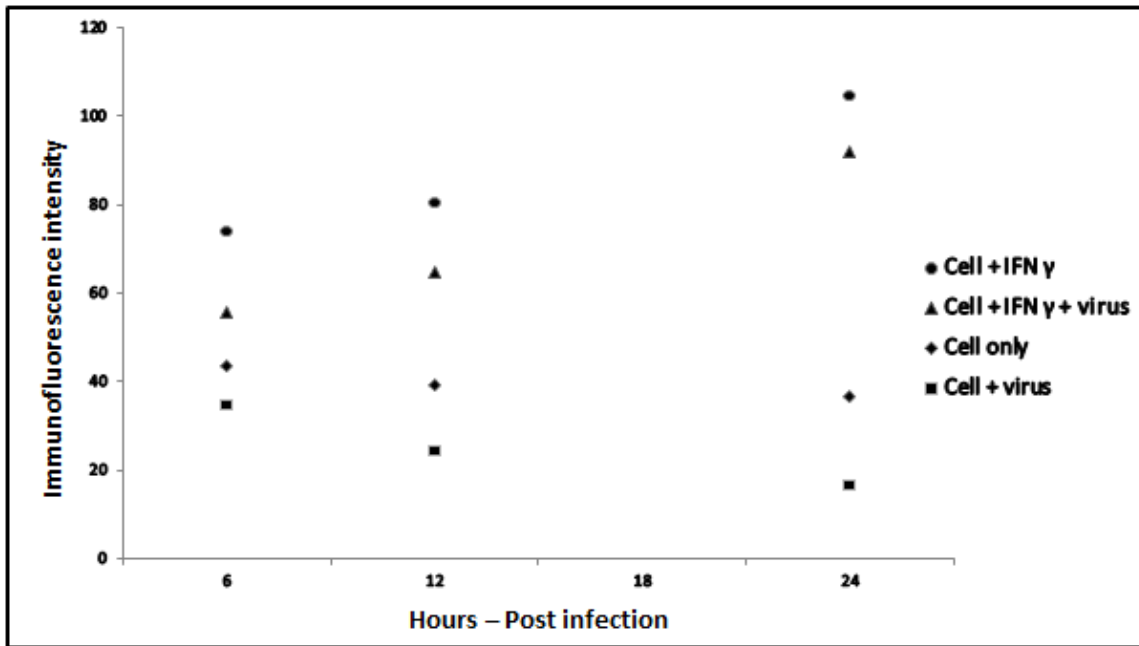


Figure 16: Comparison of MHC class I fluorescent Intensity using image J program for A2R1 fibroblasts at 6, 12 and 24 hours post infection time points. At 6, 12 and 24 hours post infection, a significant increase in the MHC class I fluorescence intensity was observed ($P < 0.001$ by ANOVA) in the cells pretreated with IFN- γ and infected with HSV-1 when compared to infected cells.

MHC class I immunofluorescence intensity by flow cytometry:

Flow cytometry was performed for all four cell lines, fibroblasts (A2R1 and L929) and keratinocytes (PAM-212 & HEL-30) at 24 hours post infection time point. Initially three experiments for each cell line were performed, taking the samples from same cell culture plate, and later three individual experiments were performed taking the samples from three different cell culture plates.

For all the Flow cytometry graphs, isotype control (purple shaded) was included in the graph. Furthermore, statistical analysis for mean fluorescence values of the MHC class I was performed through One-way Anova using Sigma plot 12.0. All the groups

passed normality test and equal variance test. Significant differences were observed between all treated groups of fibroblasts and keratinocytes and the p value was <0.001.

MHC class I immunofluorescence intensity by flow cytometry for L929 fibroblasts :

After 24 hours post infection in treated L929 fibroblasts, there was an increase in the MHC class I mean fluorescence intensity in IFN- γ pretreated cells. Cells pretreated with IFN- γ showed 4.5 fold increase in mean fluorescence compared with untreated cells (Figure 17 & 18). The HSV-1 infected cells were rescued from the infection upon IFN- γ pretreatment.

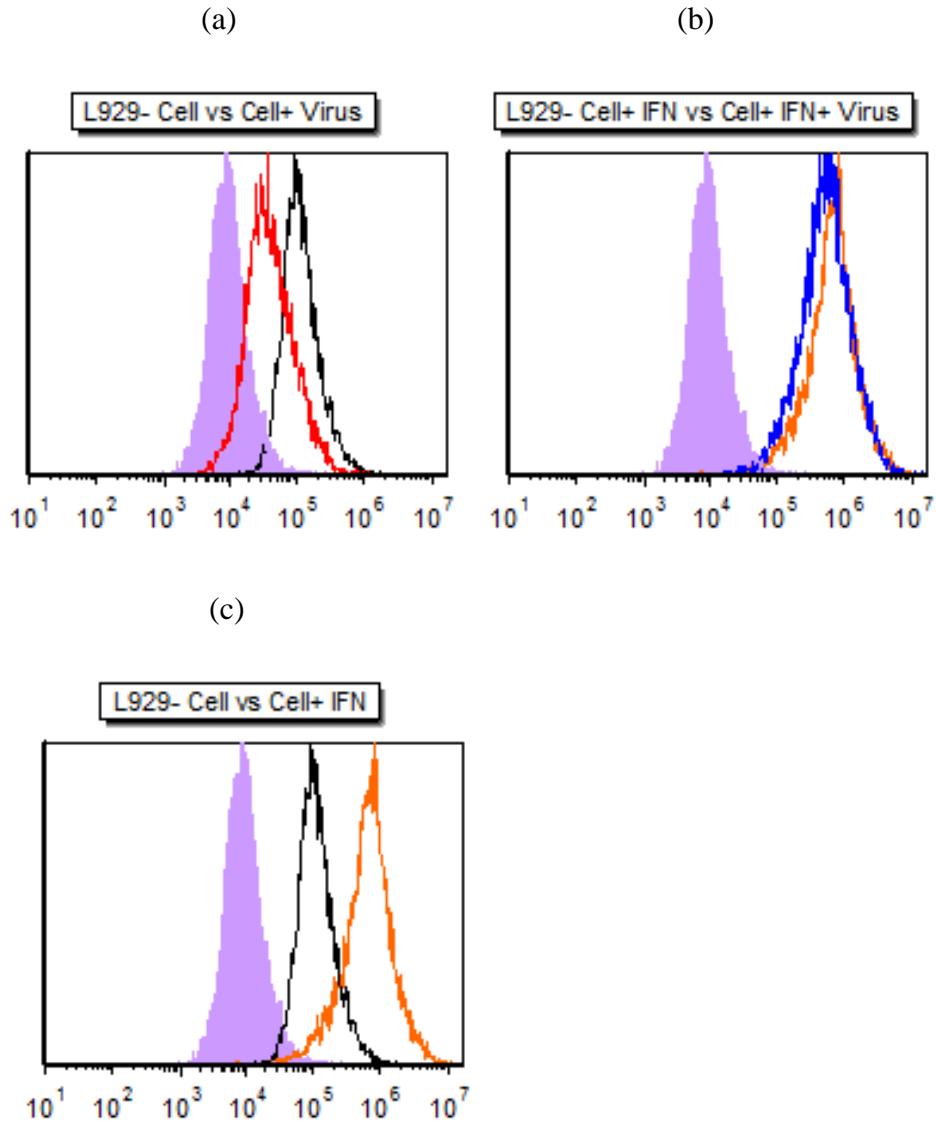


Figure 17: Major histocompatibility complex class I antigen expression for L929 fibroblasts through flow cytometry. Fluorescence-activated cell sorting analysis of HSV-1-infected cells (red) compared with uninfected cells (black) (a), IFN- γ pretreated and HSV-1-infected cells (blue) compared with IFN- γ pretreated and uninfected (orange) (b). IFN- γ -pretreated (orange) compared with untreated cells (black) (c). Isotype control (purple filled) was included in all groups but with no change in fluorescence. At 24 hours post infection, an increase in the MHC class I fluorescence intensity was observed in the cells pretreated with IFN- γ and infected with HSV-1 when compared with infected cells. Each histogram represents data for 10^6 cells. X axis = log fluorescence intensity, Y axis = number of events.

Statistical analysis was performed for mean fluorescence values of MHC class I fluorescence intensity using One-way Anova analysis using Sigma plot 12.0. There was a statistically significant difference between all treated groups for L929 fibroblasts. The p value is <0.001 (Figure 18).

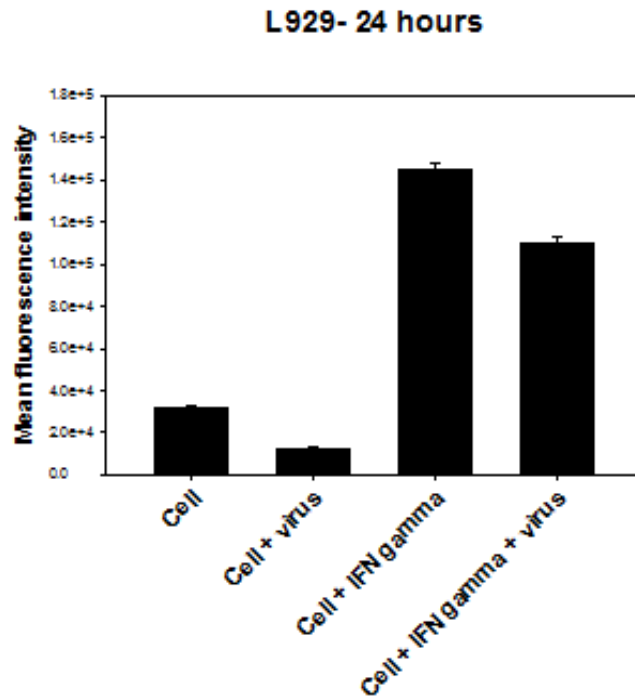


Figure 18: L929 fibroblasts- Graph for flow cytometry mean fluorescent values at 24 hours post infection. Each bar represents average of three values. Values are taken from three different experiments. At 24 hours post infection, a significant increase in the MHC class I fluorescence intensity was observed (P<0.001 by ANOVA) in the cells pretreated with IFN- γ and infected with HSV-1 when compared to infected cells.

MHC class I immunofluorescence intensity by flow cytometry for A2R1 fibroblasts:

After 24 hours post infection, a significant increase in the MHC class I mean fluorescence intensity was observed in IFN- γ pretreated cells compared to untreated cells. IFN- γ pretreatment led to a 3 fold increase in mean fluorescence compared with untreated

cells (Figure 19 & 20). The HSV-1 infected cells were rescued from the infection upon IFN- γ pretreatment.

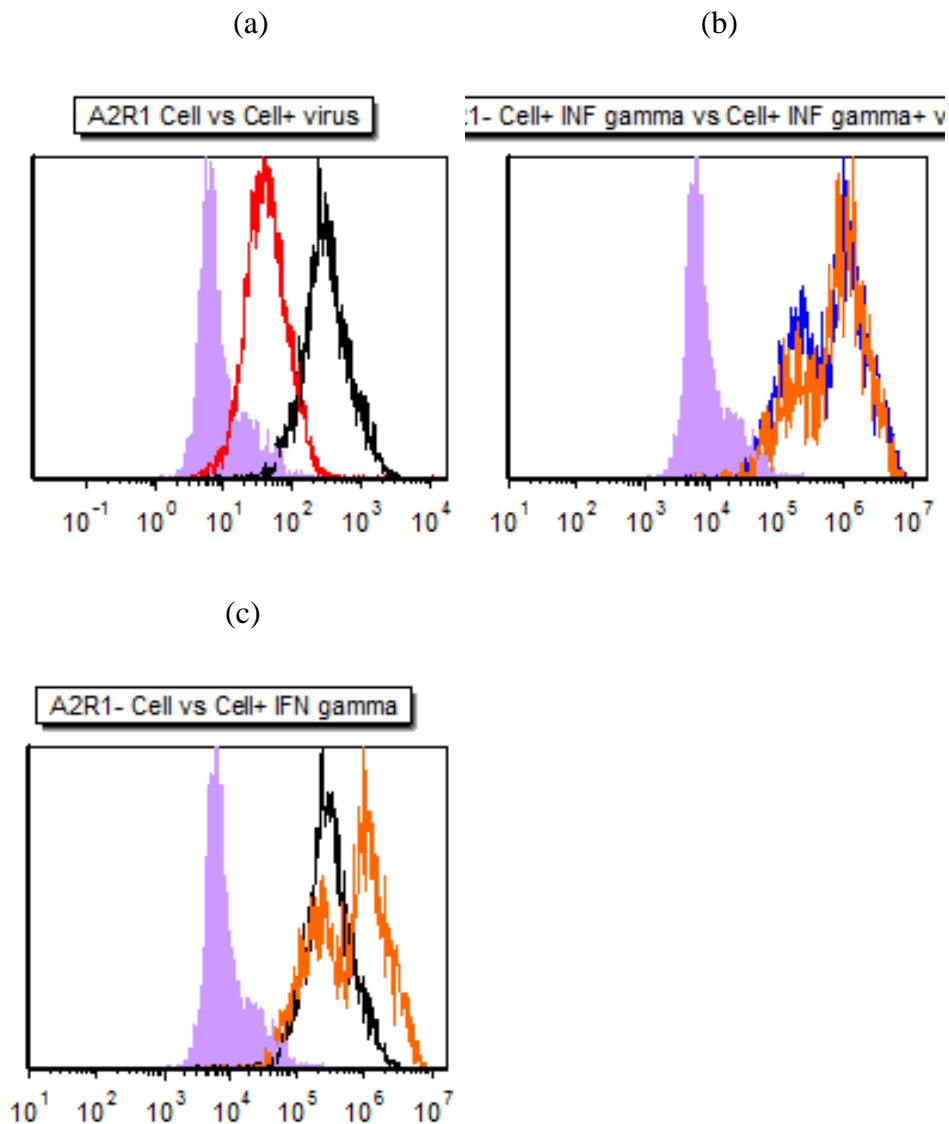


Figure 19: Major histocompatibility complex class I antigen expression for A2R1 fibroblasts through flow cytometry. Fluorescence-activated cell sorting analysis of HSV-1-infected cells (red) compared with uninfected cells (black) (a), IFN- γ pretreated and HSV-1-infected cells (blue) compared with IFN- γ pretreated and uninfected (orange) (b). IFN- γ -pretreated (orange) compared with untreated cells (black) (c). Isotype control (purple filled) was included in all groups but with no change in fluorescence. At 24 hours post infection, an increase in the MHC class I

fluorescence intensity was observed in the cells pretreated with IFN- γ and infected with HSV-1 when compared with infected cells. Each histogram represents data for 10^6 cells. X axis = log fluorescence intensity, Y axis = number of events.

Statistical analysis was performed for mean fluorescent values of MHC class I fluorescence intensity using One-way Anova analysis using Sigma plot 12.0. There was a statistically significant difference between all treated groups for A2R1 fibroblasts. The p value was <0.001 (Figure 20).

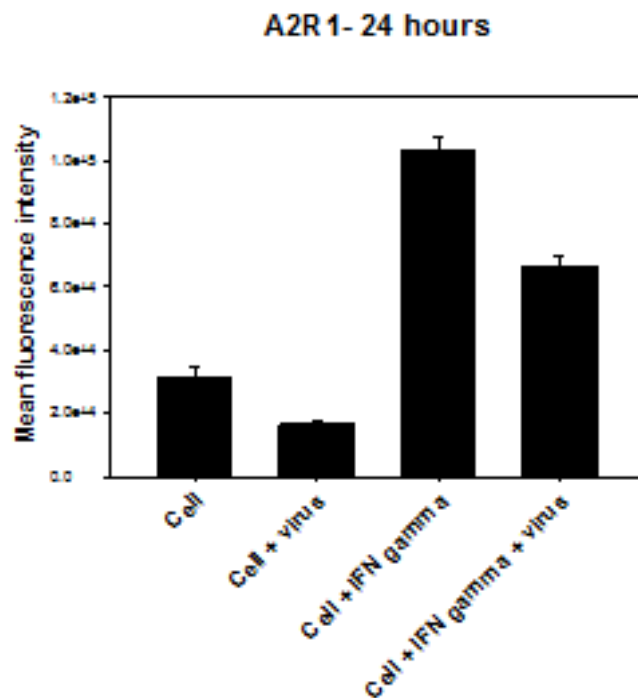


Figure 20: A2R1 fibroblasts- Graph for flow cytometry mean fluorescent values at 24 hours post infection. Each bar represents average of three values. Values are taken from three different experiments. At 24 hours post infection, a significant increase in the MHC class I fluorescence intensity was observed ($P<0.001$ by ANOVA) in the cells pretreated with IFN- γ and infected with HSV-1 when compared to infected cells.

MHC class I immunofluorescence intensity by flow cytometry for PAM-212 keratinocytes :

After 24 hours post infection in PAM-212 keratinocytes, IFN- γ pretreated cells expressed 1 fold increase in mean fluorescence compared with untreated cells. The HSV-1 infected cells expressed relatively less intensity than the cell only. IFN- γ pretreated and HSV-1 infected cells showed a slight raise in intensity but not up to the basal level like untreated cells, and the cells were not rescued from the infection (Figure 21 & 22).

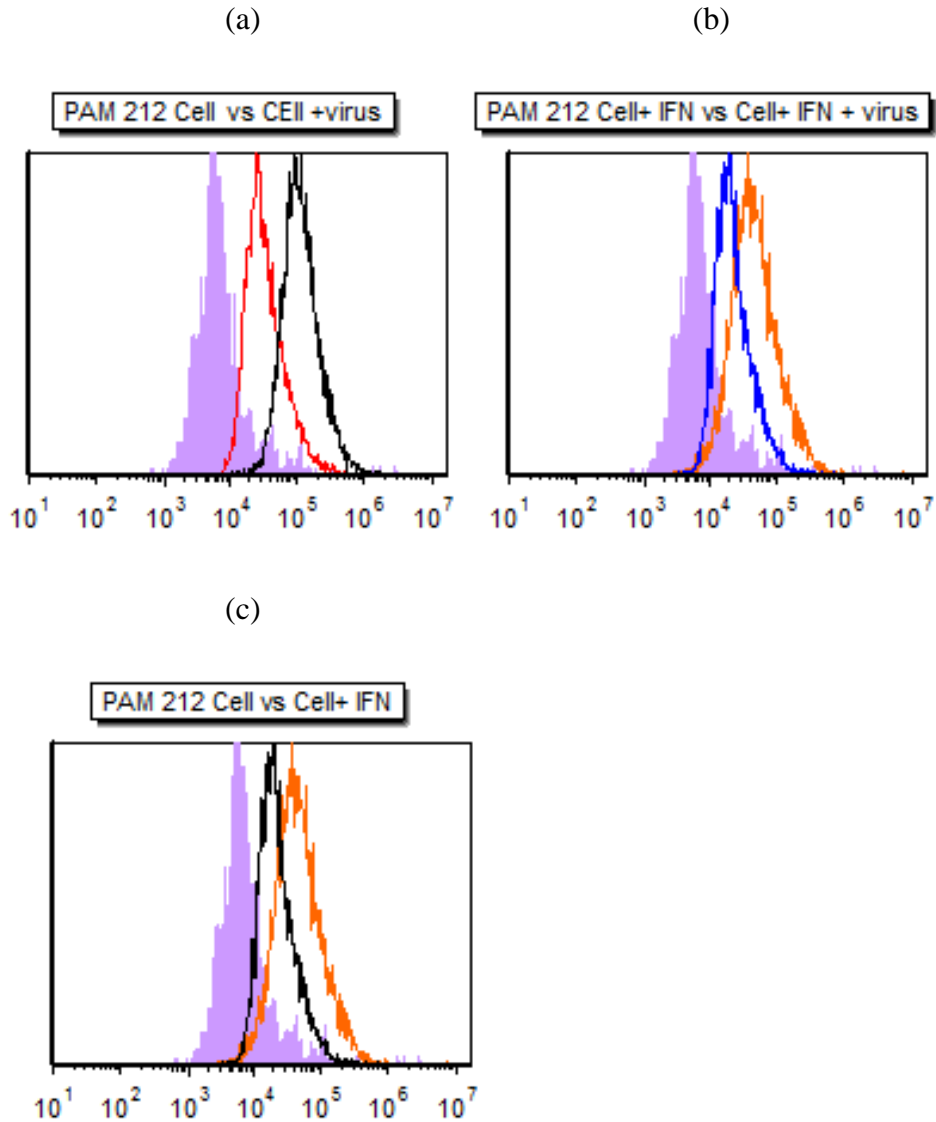


Figure 21: Major histocompatibility complex class I antigen expression for PAM-212 keratinocytes through flow cytometry. Fluorescence-activated cell sorting analysis of HSV-1-infected cells (red) compared with uninfected cells (black) (a), IFN- γ pretreated and HSV-1-infected cells (blue) compared with IFN- γ pretreated and uninfected (orange) (b). IFN- γ - pretreated (orange) compared with untreated cells (black) (c). Isotype control (purple filled) was included in all groups but with no change in fluorescence. At 24 hours post infection, a significant increase in the MHC class I fluorescence intensity was observed in the cells pretreated with IFN- γ when compared with control cells. Each histogram represents data for 10^6 cells. X axis = log fluorescence intensity, Y axis = number of events.

Statistical analysis was performed for mean fluorescence values of MHC class I fluorescence intensity using One- way Anova analysis on Sigma plot 12.0. There was a statistically significant difference between all treated groups for PAM-212 keratinocytes. p value was <0.001 (Figure 22).

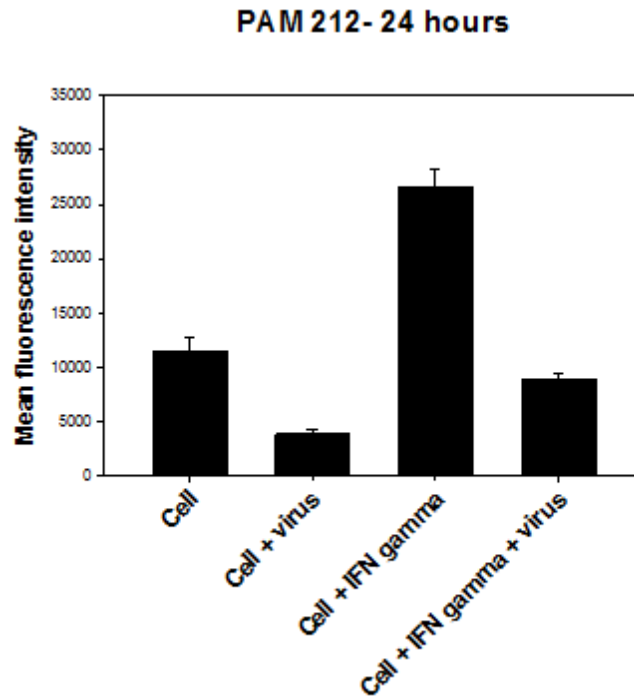


Figure 22: PAM-212 keratinocytes- Graph for flow cytometry mean fluorescent values at 24 hours post infection. Each bar represents average of three values. Values are taken from three different experiments. At 24 hours post infection, a significant increase in the MHC class I fluorescence intensity was observed ($P < 0.001$ by ANOVA) in the cells pretreated with IFN- γ when compared to control cells.

MHC class I intensity by Flow cytometry for HEL-30 keratinocytes :

After 24 hours of infection in HEL-30 keratinocytes, IFN- γ pretreated cells expressed one fold increase in mean fluorescence compared to the untreated cells; this

was similar to the results obtained for other keratinocyte PAM-212. IFN- γ pretreated and HSV-1 infected cells expressed an increase in fluorescence intensity compared with HSV-1 infected cells, but this increase was not up to the basal level of untreated cells and the cells were not protected from the infection. Both keratinocytes expressed similar pattern of MHC class I expression for the test groups but HEL-30 cells showed more susceptibility to HSV-1 infection (Figure 23 & 24).

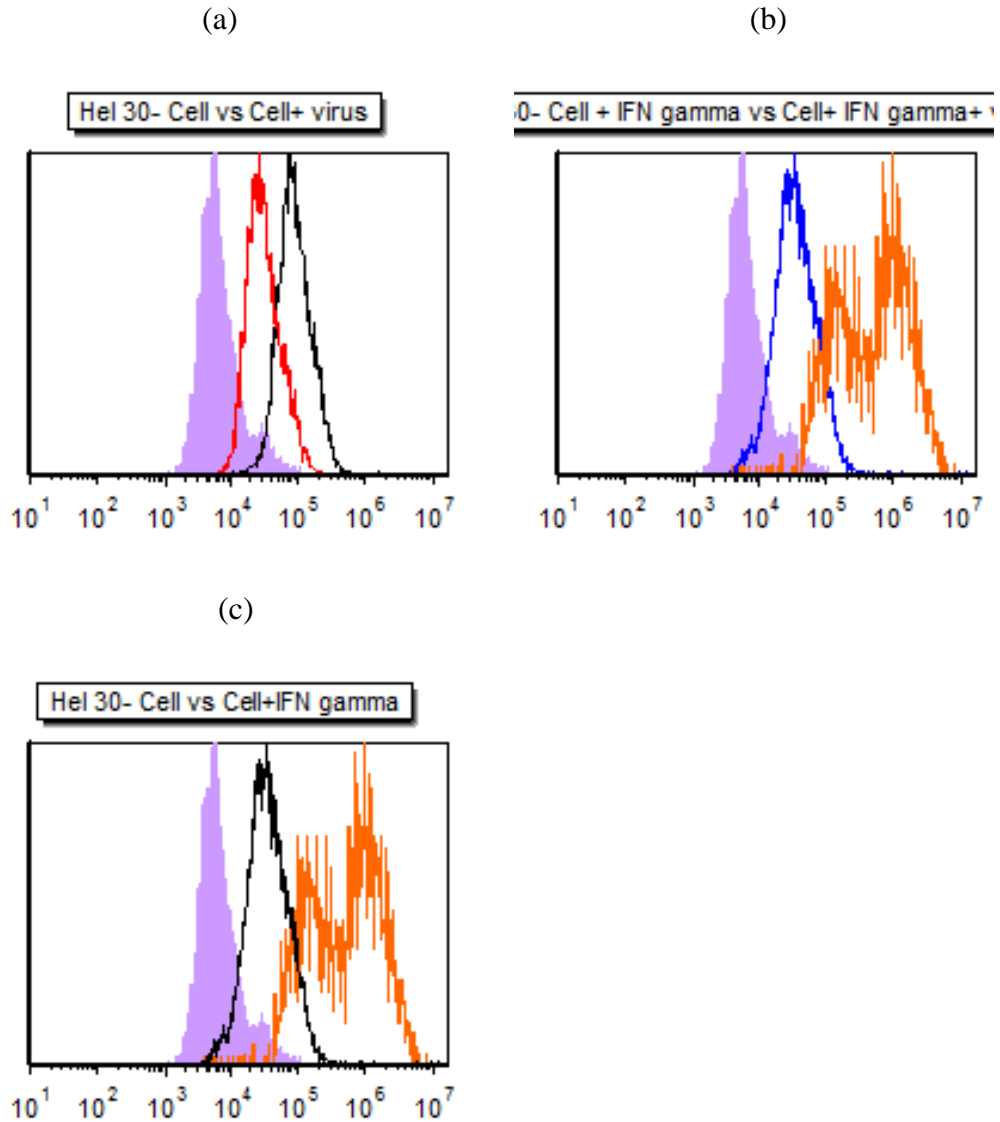


Figure 23: Major histocompatibility complex class I antigen expression for HEL-30 keratinocytes through flow cytometry. Fluorescence-activated cell sorting analysis of HSV-1-infected cells (red) compared with uninfected cells (black) (a), IFN- γ pretreated and HSV-1-infected cells (blue) compared with IFN- γ pretreated and uninfected (orange) (b). IFN- γ - pretreated (orange) compared with untreated cells (black) (c). Isotype control (purple filled) was included in all groups but with no change in fluorescence. At 24 hours post infection, a significant increase in the MHC class I fluorescence intensity was observed in the cells pretreated with IFN- γ when compared to control cells. Each histogram represents data for 10^6 cells. X axis = log fluorescence intensity, Y axis = number of events.

Statistical analysis was performed for mean fluorescence values of the MHC class I fluorescence intensity using One- way Anova analysis on Sigma plot 12.0. There was a statistically significant difference between all treated groups for HEL-30 keratinocytes. p value was <0.001(Figure 24).

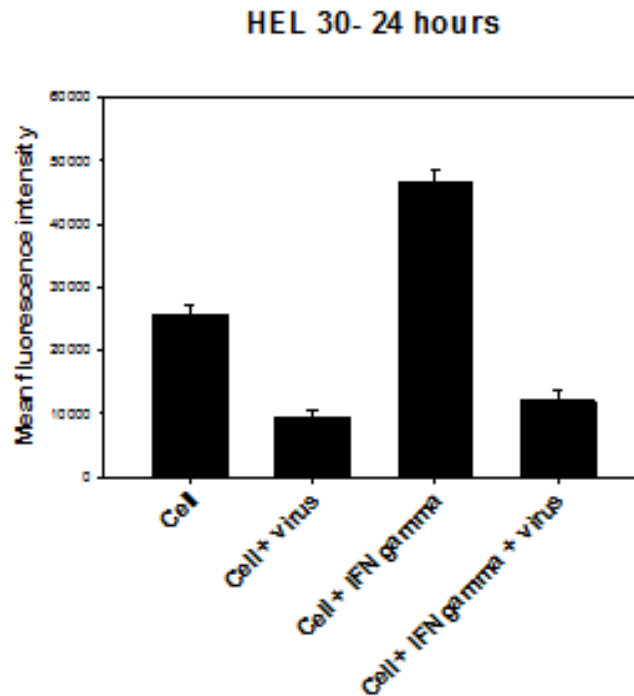


Figure 24: HEL-30 keratinocytes- Graph for flow cytometry mean fluorescent values at 24 hours post infection. Each bar represents average of three values. Values are taken from three different experiments. At 24 hours post infection, a significant increase in the MHC class I fluorescence intensity was observed (P<0.001 by ANOVA) in the cells pretreated with IFN- γ when compared to control cells.

The flow cytometry data for the fibroblasts and keratinocytes was summarized in Table 3. In this table, treated and infected groups were compared with control group and indicated the variations in MHC class I fluorescence intensity.

	A2R1	L929	PAM-212	HEL-30
Cell+ virus	Decreased	Decreased	Decreased	Decreased
Cell+ IFN-γ	Increased	Increased	Increased	Increased
Cell+ IFN-γ + virus	Increased	Increased	Decreased	Decreased

Table 3: Flow cytometry results summary for Fibroblasts (L929 & A2R1) and Keratinocytes (HEL-30 & PAM-212) compared with only cells (control) at 24 hours post infection.

DISCUSSION

In the current study, a difference was observed in the viral effects of IFN- γ on fibroblast (L929) compared to keratinocyte (HEL-30) cell lines derived from C3H mice. L929 fibroblasts were rescued from HSV-1 induced down regulation of MHC class I (Figure 17 & 18) while the HEL-30 keratinocytes were not protected (Figure 23 & 24). The induction of MHC class I by IFN- γ following HSV-1 infection of another murine keratinocyte cell line derived from BALB/c mice (PAM-212), was similar to that seen in HEL-30 cells (Figure 21 & 22). Similar to L929 cells, a fibroblast cell line from BALB/c mice (A2R1) was protected from HSV-1 induced down regulation of MHC class I (Figure 19 & 20).

Keratinocytes activated by IFN- γ pretreatment exhibited MHC class I, MHC class II and ICAM-1 expression (Mikloska et al., 1996; Mikloska and Cunningham, 1998). These factors are important for cell survival during infection. If IFN- γ action is inhibited, virus can readily infect the cells. Frey et al.,(2009) observed that IFN- γ pretreatment permitted survival of fibroblasts when infected with HSV-1 at 0.1 MOI. Fibroblasts and keratinocytes lost viability by 48 hours after infection with 0.1 MOI of HSV-1. Frey also observed an increase in expression of SOCS-1, which is a negative regulator of IFN- γ , during HSV-1 infection in keratinocytes (Frey et al., 2009). In the current study, HSV-1 infected keratinocytes alone expressed significantly less MHC class I, compared with untreated cells by 24 hours post infection (Figure 21, 22, 23 & 24). Down

regulation of MHC class I expression during virus infection probably results from cell death during infection. To account for this, a cell viability count should be performed before analyzing the samples in flow cytometry. In the current study, virus infected cells (Figure 7(b), 9(b)) expressed less MHC class I seen in immunofluorescence stained images compared with cell only (Figure 7(a), 9(a)). There was a decrease in MHC class I expression in virus infected cells.

In this study, Immunofluorescent staining for expression of MHC class I molecules in IFN- γ treated and HSV-1 infected cells was performed using two methods, namely, immunocytochemistry and flow cytometry. Only the fibroblast cell lines could be examined by both methods. To analyze immunofluorescence intensity of immunocytochemistry images, Image J software was used.

In fact of the methods, at 24 hour post infection of L929 cells, the IFN- γ treated cells increased expression of MHC class I. A 4.5 fold increase in fluorescence intensity was observed with flow cytometry (Figure 17 & 18), whereas 1.5 fold increase was seen with Image J software quantification of immunofluorescence, compared to untreated cells (Figure 10(c)).

A similar pattern resulted with A2R1 fibroblasts at 24 hours post infection. The IFN- γ treated cells showed 3 fold increase in fluorescence intensity by flow cytometry (Figure 19 & 20), whereas a 1.5 fold increase was seen with Image J software quantification of immunofluorescence, compared with untreated cells (Figure 14(c)). Similar patterns of MHC class I expression was observed using both Image J and flow cytometry quantifications, validating the use of Image J analysis of fluorescence intensity for such studies.

Currently, various laboratories are using Image J as the standard software for quantification of MHC class I immunofluorescence. For example, surface MHC class I levels were quantified during coxsackie virus B3 (CVB3) infection using Image J software (Christopher et al., 2007).

In conclusion, the current results support the data presented by Frey et al., (2009). Fibroblasts are protected against HSV-1 infection by treating the cells with IFN- γ , and keratinocytes are refractory to IFN- γ treatment. The MHC I expression can be successfully up regulated in normal and infected cells of L929 (Figure 17 & 18) and A2R1 fibroblasts (Figure 19 & 20)). IFN- γ can also up regulate MHC class I expression in keratinocytes (PAM-212 (Figure 21 & 22) and HEL-30 (Figure 23 & 24)), but during HSV-1 infection, the SOCS-1 levels increased in keratinocytes (Frey et al., 2009), which can interrupt the IFN- γ signaling pathway.

The current results indicate that fibroblasts respond well to IFN- γ treatment, since the fibroblast cells (L929 & A2R1) expressed an average of 3.5 fold increase in MHC class I expression when treated with IFN- γ , whereas keratinocytes expressed a 1-fold increase. The possible reasons can be the expression of higher levels of endogenous SOCS-1 in keratinocytes when compared with fibroblast cells (Frey et al., 2009). Frey et al. (2009) also observed that IFN- γ itself up regulates SOCS-1 expression in keratinocytes. In his study SOCS inhibitors were used in order to increase the cell survival in IFN- γ treated and HSV-1 infected keratinocytes (Frey et al., 2009).

In future studies, use of SOCS-1 inhibitors along with IFN- γ treatments for keratinocytes would be appropriate to increase the MHC class I expression during HSV-1

infection. Identification of the mRNA levels of the MHC class I protein through the RT-PCR technique would validate the results.

HSV-1 evades immune system through SOCS-1 by blocking the JAK/STAT pathway; this is an efficient way to suppress the host defense reaction (Miller et al., 1998). HEL-30 keratinocytes and PAM-212 keratinocytes express higher levels of endogenous SOCS-1 than fibroblast cells (Frey et al., 2009). A similar mechanism was observed by Yokota et al. (2004) during studies with SOCS-3 and demonstrated that IFN- α signal transduction pathway was blocked in JAK phosphorylation site in the same way as SOCS-1. Western blot revealed that STAT1 phosphorylation was inhibited in SOCS-3 over expressed FL cells. These results showed that HSV-1 also stimulates SOCS-3 expression as its anti-viral function (Yokota et al., 2004).

Although SOCS proteins play an important role in inhibition of host anti-viral defense mechanisms, it is not the only strategy stimulated by HSV-1. Lin et al. (2004) demonstrated that other strategies which do not depend on IFN- γ , can be used by HSV-1 to defeat host antiviral defense. They observed that the HSV-1 immediate early protein-ICP0 and virus shut off protein together act against immune response. Therefore, further research is required to verify which of these strategies are more effective to block host immune response by HSV-1. This could be considered as one limitation on this approach and would be an appropriate subject for future studies.

In addition, HSV-1 blocks the signaling effects of type 1 interferons by reducing the effects of the double-stranded RNA-activated protein kinase (PKR) (Melroe et al., 2004). Frey et al. (2009) mentioned that treatment of cells with IFN- β and IFN- γ inhibits

viral replication and mRNA accumulation to a greater extent than treatment with either IFN alone. IFN- γ can also be used in combination of type 1 interferons.

For future studies, it would be of interest to verify whether the combinations of interferons exert changes in SOCS-1 levels through Western blot technique, assessing mRNA levels using RT-PCR, while simultaneously measuring MHC class I expression levels.

Frey et al. (2009) observed that keratinocytes (HEL-30) were refractory to IFN- γ induction of an antiviral state during HSV-1 infection. Refractiveness of keratinocytes to IFN- γ was attributed to the production of SOCS-1. Both IFN- γ and HSV-1 were found to up regulate production of SOCS-1 in keratinocytes. Identifying whether SOCS-1 inhibitors would permit the keratinocytes to express any type I interferon response and protect the cells from HSV-1 induced MHC class I down regulation would be analyzed.

Recent studies have demonstrated that keratinocytes are capable of producing pro-inflammatory cytokines in response to virus infection (Hukkanen et al., 2002). Production of IL-1 β , TNF- α and IL-6 was observed during HSV-1 infection of primary keratinocytes from BALB/C and C57Bl/6 mice (Sprecher and Becker, 1992). Fibroblasts also have immune functions. Particularly, fibroblasts secrete pro-inflammatory cytokines that mediate extravasation of leukocytes (McGettrick et al., 2009). Determination of these secretory cytokines prior and post virus infection would give further insight on inflammatory response following virus infection and the influence of these cytokines on the MHC class I expression levels. A brief experimental design is proposed for measuring type 1 interferons during HSV-1 infection in few steps:

1. Infected cells could be lysed, and IFN- β levels measured using a murine IFN- β ELISA kit (Ahmed et al., 2010). IFN- α can be measured using IFN- α ELISA kit (Fujisawa et al., 1997). Using cell lysates for measuring IFN levels would show the IFN response to early infection. Culture supernatant fluids of fibroblast and keratinocyte cells can also be analyzed for IFN- β , and IFN- α production (Fujisawa et al., 1997).
2. Measuring the IFN levels before infection would show the actual amounts produced post infection.
3. Fluorescently labeled anti mouse IFN antibodies can be used if the ELISA kits are not sensitive enough to detect interferons.
4. Western blot technique can be used to measure protein levels (interferon levels).
5. Further validations can be done by detecting mRNA levels for these interferons through RT PCR.

REFERENCES

1. Akhtar J, Tiwari V, Oh MJ, et al. (2008). HVEM and nectin-1 are the major mediators of herpes simplex virus 1 (HSV-1) entry into human conjunctival epithelium. *Invest Ophthalmol Vis Sci*, 49(9); 4026–35.
2. Ansel, J., Perry, P., Brown, J., Damm, D., Phan, T., Hart, C., Luger, T., and Hefeneider, S. (1990). Cytokine modulation of keratinocyte cytokines. *J Invest Dermatol*, 94; 101S-107S.
3. Armerding, D., and Rossiter, H. (1981). Induction of natural killer cells by herpes-simplex virus type 2 in resistant and sensitive inbred mouse strains. *Immunobiology*, 158; 369-379.
4. Bach, E. A., Aguet, M., Schreiber, R. D. (1997). The IFN gamma receptor: a paradigm for cytokine receptor signaling. *Annu Rev Immunol*, 15; 563-91.
5. Chmielarczyk, W., Domke, I., and Kirchner, H. (1985). Role of interferon in the resistance of C3H/HeJ mice to infection with herpes simplex virus. *Antiviral Res*, 5; 55-59.
6. Christopher T. Cornell, William B. Kiosses, Stephanie Harkins and J. Lindsay Whitton. (2007). Coxsackievirus B3 Proteins Directionally Complement Each Other To Downregulate Surface Major Histocompatibility Complex Class I. *J Virol*, 81; 6785–6797.
7. Engler, H., Zawatzky, R., Kirchner, H., and Armerding, D. (1982). Experimental infection of inbred mice with herpes simplex virus. IV. Comparison of interferon production and natural killer cell activity in susceptible and resistant adult mice. *Arch Virol*, 74; 239-247.

8. Favoreel, H.W., Nauwynck, H.J., and Pensaert, M.B. (2000). Immunological hiding of herpesvirus-infected cells. *Arch Virol*, 145; 1269-1290.
9. Fujisawa, H., Kondo, S., Wang, B., Shivji, G. M., & Sauder, D. N. (1997). The expression and modulation of IFN-alpha and IFN-beta in human keratinocytes. *J Interferon & Cytokine Res*, 17(12); 721-725.
10. Frey, K. G., Ahmed, C. M., Dabelic, R., Jager, L. D., Noon-Song, E. N., Haider, S. M., & Bigley, N. J. (2009). HSV-1-induced SOCS-1 expression in keratinocytes: Use of a SOCS-1 antagonist to block a novel mechanism of viral immune evasion. *J Immunol*, 183(2); 1253-1262.
11. Frey, K. G. (2009). (Unpublished Ph.D. Thesis). Wright State University.
12. Gregory T. Melroe, Neal A. DeLuca and David M. Knipe. (2004). Herpes Simplex Virus 1 Has Multiple Mechanisms for Blocking virus-Induced Interferon Production. *J Virol*, 78(16); 8411-20.
13. Hukkanen, V., Broberg, E., Salmi, A., and Eralinna, J.P. (2002). Cytokines in experimental herpes simplex virus infection. *Int Rev Immunol*, 21; 355-371.
14. Isaacs, A., Lindermann, J. (1957). Virus interference. I. The interferon. *Proc. R. Soc. Lond. B Biol Sci*, 147; 258-26.
15. Jaroszeski MJ, Radcliff G. (1999). Fundamentals of flow cytometry. *Mol Biotechnol*, 11(1); 37-53.
16. Knickelbein, J., Khanna, K., Yee, M., Catherine, B., Kinchington, P., Hendricks R. (2008). Noncytotoxic lytic granule-mediated CD8+ T cell inhibition of HSV-1 reactivation from neuronal latency (supporting online material). *Science*, 322; 268–271.

17. Lacaille, V.G., and Androlewicz, M.J. (1998). Herpes simplex virus inhibitor ICP47 destabilizes the transporter associated with antigen processing (TAP) heterodimer. *J Biol Chem*, 273; 17386-17390.
18. Ladwein M, Rottner K. (2008). On the Rho'd: the regulation of membrane protrusions by Rho-GTPases. *FEBS Lett*, 582(14); 2066–74.
19. Lin, R., R.S. Noyce, S. E. Collins, R. D. Everett, and K. L. Mossman. (2004). The herpes simplex virus ICP0 ring finger Domain Inhibits IRF3- and IRF7- mediated activation of interferon-stimulated Genes. *J Virol*, 78; 1675-1684.
20. Marshall DS, Linfert DR, Draghi A, McCarter YS, Tsongalis GJ. (2001). Identification of herpes simplex virus genital infection: comparison of a multiplex PCR assay and traditional viral isolation techniques. *Mod Pathol*, 14; 152–156.
21. McGettrick, H.M., Smith, E., Filer, A., Kissane, S., Salmon, M., Buckley, C.D., Rainger, G.E., and Nash, G.B. (2009). Fibroblasts from different sites may promote or inhibit recruitment of flowing lymphocytes by endothelial cells. *Eur J Immunol*, 39; 113-125.
22. Mellman I and Steinman RM. (2001). Dendritic cells: specialized and regulated antigen processing machines. *Cell*, 106; 255–25.
23. Melroe, G.T., DeLuca, N.A., and Knipe, D.M. (2004). Herpes simplex virus 1 has multiple mechanisms for blocking virus-induced interferon production. *J Virol*, 78; 8411-8420.
24. Mikloska, Z., and Cunningham, A.L. (1998). Herpes simplex virus type 1 glycoproteins gB, gC and gD are major targets for CD4 T-lymphocyte

- cytotoxicity in HLA-DR expressing human epidermal keratinocytes. *J Gen Virol*, 79; 353-361.
25. Mikloska, Z., Bosnjak, L., and Cunningham, A.L. (2001). Immature monocyte-derived dendritic cells are productively infected with herpes simplex virus type 1. *J Virol*, 75; 5958-5964.
26. Mikloska, Z., Danis, V.A., Adams, S., Lloyd, A.R., Adrian, D.L., and Cunningham, A.L. (1998). In vivo production of cytokines and beta (C-C) chemokines in human recurrent herpes simplex lesions--do herpes simplex virus-infected keratinocytes contribute to their production. *J Infect Dis*, 177; 827-838.
27. Miller, D. M., B. M. Rahill, J. M. Boss, M. D. Lairmore, J. E. Durbin, J. W. Waldman, and D. D. Sedmak. (1998). Human cytomegalovirus inhibits major histocompatibility complex class II expression by disruption of the Jak/Stat pathway. *J Exp Med*, 187; 675-683.
28. Minami M., Kita M., Yan X., Yamamoto T., Iida T., Sekikawa K., Iwakura Y., Imanishi J. (2002). Role of IFN- γ and Tumor Necrosis Factor- α in Herpes Simplex Virus Type 1 Infection. *J Interferon & Cytokine Res*, 22(6); 671-676.
29. Mikloska, Z., Kesson, A.M., Penfold, M.E., and Cunningham, A.L. (1996). Herpes simplex virus protein targets for CD4 and CD8 lymphocyte cytotoxicity in cultured epidermal keratinocytes treated with interferon-gamma. *J Infect Dis*, 173; 7-17.
30. Minagawa, H., Hashimoto, K., and Yanagi, Y. (2004). Absence of tumour necrosis factor facilitates primary and recurrent herpes simplex virus-1 infections. *J Gen Virol*, 85; 343-347.

31. Nicola, A.V., Hou, J., Major, E.O., and Straus, S.E. (2005). Herpes simplex virus type 1 enters human epidermal keratinocytes, but not neurons, via a pH-dependent endocytic pathway. *J Virol*, 79; 7609-7616.
32. Nina Korzeniewski, Rolando Cuevas, Anette Duensing, and Stefan Duensing. (2010). Daughter Centriole Elongation Is Controlled by Proteolysis. *Mol Biol Cell*, 21; 3942-3951.
33. Norkin, L. C. (2010). *Virology* (First ed.). Washington, D.C.: ASM Press, pp 471.
34. Oh MJ, Akhtar J, Desai P, Shukla D. (2010). A role for heparan sulfate in viral surfing. *Biochem Biophys Res Commun*, 391(1); 176–81.
35. Pena KC, Adelson ME, Mordechai E, Blaho JA. (2010). Genital herpes simplex virus type 1 in women: detection in cervicovaginal specimens from gynecological practices in the United States. *J Clin Microbiol*, 48; 150–153.
36. Perera, R.J., Koo, S., Bennett, C.F., Dean, N.M., Gupta, N., Qin, J.Z., and Nickoloff, B.J. (2006). Defining the transcriptome of accelerated and replicatively senescent keratinocytes reveals links to differentiation, interferon signaling, and Notch related pathways. *J Cell Biochem*, 98; 394-408.
37. Raftery MJ, Behrens CK, Miller A, Krammer PH, Walczak H, Schnrich G. (1999). Herpes Simplex Virus Type 1 Infection of Activated Cytotoxic T Cells. *J Exp Med*, 190(8); 1103–1113.
38. Rupert Abele and Robert Tempe. (2004). The ABCs of Immunology: Structure and Function of TAP, the Transporter Associated with Antigen Processing. *J Physiology*, 19; 216-24.

39. Sarah Salameh, Urmi Sheth, and Deepak Shukla. Early Events in Herpes Simplex Virus Lifecycle with Implications for an Infection of Lifetime. (2012). *J Virol*, 6; 1–6.
40. Shahin, V., Hafezi, W., Oberleithner, H., Ludwig, Y., Windoffer, B., Schillers, H., and Kuhn, J.E. (2006). The genome of HSV-1 translocates through the nuclear pore as a condensed rod-like structure. *J Cell Sci*, 119; 23-30.
41. Shukla D, Spear PG. (2001). Herpesviruses and heparan sulfate: an intimate relationship in aid of viral entry. *J Clin Invest*, 108(4); 503–10.
42. Sheridan, B. S., Knickelbein, J. E., Hendricks, R. L. (2007). CD8 T cells and latent herpes simplex virus type 1: keeping the peace in sensory ganglia. *Expert Opinion on Biological Therapy*, 7(9); 1323-31.
43. Sprecher, E., and Becker, Y. (1992). Detection of IL-1 beta, TNF-alpha, and IL-6 gene transcription by the polymerase chain reaction in keratinocytes, Langerhans cells and peritoneal exudate cells during infection with herpes simplex virus-1. *Arch Virol*, 12; 253-269.
44. Tomazin R, van Schoot NE, Goldsmith K, Jugovic P, Sempe P, et al. (1998). Herpes simplex virus type 2 ICP47 inhibits human TAP but not mouse TAP. *J Virol*, 72; 2560–2563.
45. Taylor, T.J., Brockman, M.A., McNamee, E.E., and Knipe, D.M. (2002). Herpes simplex virus. *Front Bio Sci*, 7; 752-64.
46. Lilly Cheng Immergluck, Miriam S. Domowicz, Nancy B. Schwartz and Betsy C. Herold. (1998). Viral and cellular requirements for entry of herpes simplex virus type 1 into primary neuronal cells. *J Virol*, 79; 549–559.

47. Waiboci, L. W., C. M. Ahmed, M. G. Mujtaba, L. O. Flowers, J. P. Martin, M. I. Haider, and H. M. Johnson. (2007). Both the suppressor of cytokine signaling-1 (SOCS-1) kinase inhibitory region and SOCS-1 mimetic bind to JAK2 autophosphorylation site: implications for the development of a SOCS-1 antagonist. *J Immunol*, 178; 5058-5068.
48. Watanabe, D., Adachi, A., Tomita, Y., Yamamoto, M., Kobayashi, M., and Nishiyama, Y. (1999). The role of polymorphonuclear leukocyte infiltration in herpes simplex virus infection of murine skin. *Arch Dermatol Res*, 291; 28-36.
49. Wharton, S.B., Meyers, N.L., and Nash, A.A. (1995). Experimental herpes simplex virus type 1 (HSV-1) infection of the spinal cord and dorsal root ganglia. *Neuropathol Appl Neurobiol*, 21; 228-237.
50. Whitley, R.J., and Roizman, B. (2001). Herpes simplex virus infections. *Lancet*, 357; 1513-1518.
51. Yokota, S., N. Yokosawa, T. Okabayashi, T. Suztani, S. Miura, K. Jimbow, and N. Fujii. (2004). Induction of suppressor of cytokine signaling-3 by herpes simplex type-1 contributes to inhibition of the interferon signaling pathway. *J Virol*, 78; 6282-6282